ELSEVIER

Coordination Chemistry Reviews
188 (1999) 157–210

COORDINATION CHEMISTRY REVIEWS

www.elsevier.com/locate/ccr

NMR and EPR spectroscopies and electron density distribution in polyoxoanions

L.P. Kazansky [a], B.R. McGarvey [b,*]

[a] *Institute of Physical Chemistry, Russian Academy of Sciences, 31, Leninsky pr. 117071, Moscow, Russia*

[b] *Department of Chemistry and Biochemistry, University of Windsor, Windsor, Ont, N9B 3P4, Canada*

Received 2 June 1998; received in revised form 29 September 1998; accepted 16 November 1998

Contents

* Corresponding author. Tel.: +1-519-2533000; fax: +1-519-9737098.
E-mail address: beprm@uwindsor.ca (B.R. McGarvey)

PII: S0010-8545(98)00244-6

Abstract

The results of NMR and EPR studies are considered for large polyoxoanions of molybdenum and tungsten with paramagnetic and some diamagnetic centers which produce delocalized electrons. For various polyoxoanions the possible mechanisms of electron density transfer involving π- and σ-bonding, depending on hybridization, bond lengths, and geometric configuration are analyzed. The different contributions to the observed chemical shifts including contact, pseudocontact (dipolar ligand centered), dipolar (metal centered) and spin polarization terms are considered and sometimes evaluated. Formation of the delocalized electron pair or bipolaron is proven by ^{17}O- and ^{183}W-NMR. The changes observed in the ^{183}W-NMR spectra of polyanions with non-equivalent tungsten atoms with the delocalized electron pair are believed to be due to the existence of the spin bipolaron. A model of the circulation of the electron density in $Co^{3+}W_{12}O_{40}^{5-}$ due to the dynamic Jahn–Teller effect is developed. The possibility of spin-paired electron transfer from the 3d-cation into the ligand orbitals of the nucleus under investigation is proposed.

Keywords: Polyoxoanions; Mixed valence; Delocalization of polaron and bipolaron; NMR; EPR

1. Introduction

Polyoxoanions of molybdenum and tungsten constitute an important and specific class of coordination compounds. In heteropolyanions a polyoxometalate sphere acts as a large ligand with respect to a central (hetero) atom. These polyoxoanions, due to their unique structural and electronic properties, find applications in many fields of science and technology [1–3]. In many cases when their catalytic, electrochromic and other properties are used, they participate in redox reactions with rather specific electron density transfer. Studies of the electron density distribution both in the diamagnetic and paramagnetic species are quite important for understanding the nature of the chemical bonding in heteropolyanions and their role in many chemical reaction.

NMR of different nuclei constituting a polyoxoanion is now recognized to be a very powerful method for the elucidation of the molecular structure of iso- and heteropolyanions (IPA and HPA) of vanadium, molybdenum and tungsten both in solution and sometimes in the solid state [3–5]. The ^{17}O-, ^{51}V-, and ^{183}W-NMR prove to be the most informative due to their rather narrow lines and widely spread chemical shifts, allowing the assignment of the observed lines to atoms located in

the various positions. Moreover the NMR of other nuclei which can be part of HPA such as ^{31}P, ^{29}Si, ^{71}Ga, ^{73}Ge, ^{95}Mo and others offer the possibility for study of the structure and bonding of HPA in detail.

NMR also proves to be a very valuable tool to study the electron density distribution due to the large chemical shifts induced both by paramagnetic atoms and by electron transfer between atoms in diamagnetic HPA.

EPR spectroscopy is also well suited to study delocalization problems and spin density distribution but it is limited to systems with unpaired electrons. Polyoxoanions present sometimes a situation where both complementary methods may be applied to the same paramagnetic complexes.

In this review we consider the results obtained from heteronuclear NMR spectra together with EPR data to understand the mechanisms of electron density distribution in large, fully inorganic polyoxocomplexes. Moreover in many cases the conclusions may be transferred to the mixed valence oxide systems whose structures are also based on combinations of MO_6 octahedra.

2. Theoretical background

2.1. Structure and bonding in polyoxoanions

In most cases, hexavalent molybdenum and tungsten form distorted MO_6 octahedra with common vertices, edges or sometimes faces to build a polyoxoanion. Distortion of the MO_6 skeleton is due to the intrinsic ability of molybdenum and tungsten cations to form one or two short terminal $M{=}O_d$ bonds with other oxygen atoms being used in different M–O–M bridges. Various combinations of octahedra with the bridging oxygen atoms linking two octahedra by vertex (O_b) or linking octahedra by edge (O_c) gives rise to a great variety of structures of general formula $X_xN_mO_o^{n-}$, where X is encapsulated in the polyoxometalate sphere built of oxygen atoms O_a in common with molybdenum, tungsten or vanadium.

Two major types of HPA are known: Type I is built of octahedra each having one terminal bond and Type II is built of octahedra with two terminal $M{=}O_d$ bonds [5], shown in Schemes I and II.

According to model molecular orbital (MO) calculations [6] for MO_6 octahedra of different symmetries (confirmed also by calculations for large polyoxoanions) the MO diagram, shown in Scheme I is slightly different from the generally accepted and frequently cited MO diagram proposed by Ballhausen and Gray [7] for the oxovanadyl cation. The d_σ orbitals are found to be inverted with $d_{x^2-y^2}$ being above d_{z^2}. Taking account of this, some peculiarities in the EPR spectra of reduced HPA species may be understood [8].

Polyanions of Type I are more important because they usually exhibit reversible redox reactions. Generally speaking, one terminal bond makes the local symmetry of each octahedron appear close to C_{4v} with the empty antibonding d_{xy} orbital overlapping with the $2p_\pi$ orbitals of the bridging oxygen atoms.

As shown below the bridging oxygen atoms O_b and O_c play a significant role in the electron transfer, the less bent M–O_b–M due to more favorable overlap of orbitals, gives the most effective pathway. Depending on the number of atoms which are bound to oxygen the degree and the nature of the electron transfer may vary.

The electron density may be transferred directly, e.g. using π-bonding from the M d_{xy} orbital to the p_π-orbital of the bridging oxygen atoms or may be created by a spin polarization mechanism. If a paramagnetic cation has electrons in the e_g and t_{2g} orbitals there may be at least two mechanisms for the unpaired electrons to interact with the ligand nucleus under consideration.

Unfortunately rigorous quantitative estimation of the electron density distribution is not possible at present due to the various possible pathways for electron delocalization. In most cases we restrict ourselves to a qualitative description of the electron density distributions in large polyoxoanions, based on NMR and EPR data and consider the possible mechanisms.

2.2. NMR and electron density transfer

The NMR chemical shift with diamagnetic systems in solution arises from two contributions: diamagnetic (σ_{dia}) and paramagnetic (σ_p) [9]. The diamagnetic term is determined by the potential created by the inner electrons and usually it is reasonably constant for closely related molecules. The paramagnetic contribution, which determines the variation of the observed chemical shift, arises from Zeeman mixing of the low lying excited states with the ground state and may be estimated from the Jameson-Gutowsky equation [9]:

$$\sigma_p = \frac{H - H_0}{H_0} = \frac{2e^2h^2}{3m^2c^2\Delta E}\ [\langle r^{-3}\rangle_{pu} + \langle r^{-3}\rangle_d D_u] \quad (1)$$

where P_u and D_u give the imbalance of the valence electrons in p and d orbitals belonging to the nucleus under consideration. ΔE is the average energy of the excitation. The $\langle r^{-3}\rangle_p$ and $\langle r^{-3}\rangle_d$ are the average values for the electron in the p and d orbitals of the nucleus.

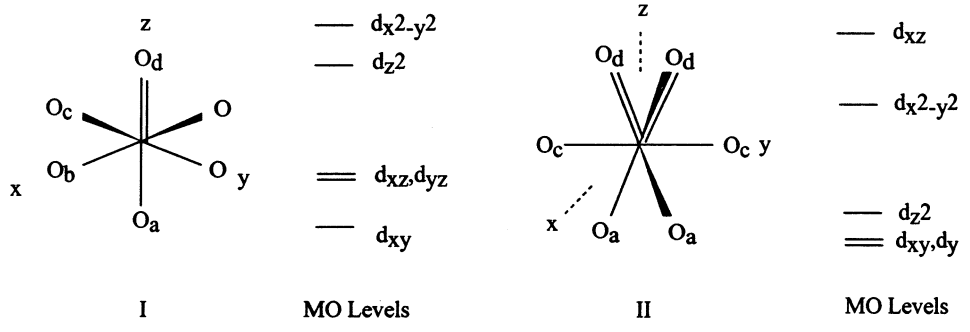

Scheme I.

Scheme II.

The importance of the paramagnetic contribution to the observed chemical shifts for a large number of closely related polyoxoanions was shown by the correlation between the ^{17}O chemical shifts [10] and ^{183}W chemical shifts [11] and the reciprocal energy, $E_{(LCT)}$, of the lowest charge transfer (LCT). However, the LCT (optical dipole allowed transition) is not responsible for σ_p and therefore some deviations from correlations are found for close but not identical polyanions.

In many cases, attribution of the observed ^{183}W-NMR lines to corresponding atoms may be made using nuclear–nuclear spin coupling $^2J_{W-W}$ connectivities [12] and NMR becomes a routine method to prove the identity of the polyoxo anions in solution [3,5].

The situation is dramatically changed if (i) the polyoxo anion contains a paramagnetic atom whether as a central atom or when it replaces one of the atoms in the coordination sphere, (ii) when the metal atoms of the coordination sphere accept electron(s) which may be localized or delocalized, or (iii) when there is a transfer of electron density from a diamagnetic cation onto neighboring atoms. Unfortunately, the isotropic shifts are sometimes quite large and vary in an unexpected manner; this presents some difficulties in their observation [13], as has been considered by Jorris et al. [14].

A well resolved paramagnetic NMR shift will be observed if the electronic relaxation rate T_{1e}^{-1}, is greater than A/h, where A is the nuclear–electron hyperfine interaction in energy units. Generally, the isotropic paramagnetic shift is separated into two components [15]. The contact term, F_c, arises from the electron–nuclear interaction in a ligand s orbital of the atom containing the nucleus whose shift is being measured. This is often called the Fermi contact shift in honour of the man who showed how an unpaired electron in the spherical s orbital could give rise to an isotropic dipole–dipole interaction between the nuclear magnetic moment and the electron magnetic moment. The contact shift, σ_c, is often given by the equation:

$$\sigma_c = \frac{H - H_0}{H_0} = \frac{A_S}{(\gamma_N/2\pi)h} \frac{\langle S_z \rangle}{H_0} \tag{2a}$$

where $\langle S_z \rangle$ is the thermal average of the electron spin operator over all spin states, A_s is the isotropic part of the hyperfine constant, and γ_N is the magnetogyric ratio of the nucleus. If the ground state is a simple state of total spin S this equation further simplifies to:

$$\sigma_c = -\frac{g\beta S(S+1)}{(\gamma_N/2\pi)h} \frac{A_s}{3kT} \tag{2b}$$

where g is the rotationally averaged g-value, β is the Bohr magneton and k is the Boltzmann constant. Eq. (2b) is incorrect if there is a zero field splitting $\geq kT$ and Eq. (2a) is incorrect if A_s is not identical for the states averaged over, which could occur for orbitally degenerate ground states and all f^n systems.

For transition metal ions, spin transfer to the ligand atoms is predominantly through the covalent interaction between metal d orbitals and s, p, or d ligand orbitals. If symmetry allows direct admixture of s orbitals into the MO then (A_s/γ_N) is positive and proportional to density of the unpaired spin in the s orbital. Spin

transfer into ligand p and d orbitals can also produce a smaller magnitude A_s through a spin-polarization mechanism and this A_s is generally negative in sign. Transition metal systems with orbitally degenerate ground states, such as octahedral d^6, tetrahedral d^7, strong field octahedral d^5, etc., do not satisfy the assumptions made in Eq. (2a) and need to be more thoroughly examined theoretically. An attempt to do this has been made recently [16].

For lanthanide and actinide metals the problem is somewhat altered due to the fact that the spin–orbit interaction is larger than the ligand field interaction for the f orbitals. For the lanthanides the 4f orbitals are buried deep in the ion and the outer valence shell is mainly 6s and 6p. Covalent interactions of 4f electrons is very small as evidenced by the small ligand field splittings observed. For the lanthanides, one must consider another mechanism of spin transfer from the lanthanide ion to the ligand atoms called the polarization mechanism. It has been shown that exchange interactions in the lanthanide ion produce a polarization of spin in the outer 6s, 6p shell of opposite sign to that of the f electrons. Since these electrons are likely to have much stronger covalent interactions with neighbouring ligand atoms it is possible for the main spin transfer mechanism to be this one which transfers spin of opposite sign which in turn will produce a NMR shift opposite in sign to that produced by a covalent spin transfer from the f orbitals. It has been demonstrated that the polarization mechanism often dominates but not in every system. It would be expected that more covalency is likely for actinide 5f orbitals and this is confirmed by the larger ligand field splittings observed for some actinide systems. Thus the covalent transfer could be seen more often in these systems. It is of interest to note [17] that $\langle S_z \rangle / H$ is positive for lanthanide ions in the earlier part of the periodic series and becomes negative in the later part of the series.

For clarity note that $\sigma = \Delta H / H_0$ is positive for upfield shifts (nucleus is more shielded) and that $\sigma = -\delta$, where $\delta = (\nu - \nu_0)/\nu_0$ and is the chemical shift (in ppm) referred to in the Tables.

When the angular momentum component of the magnetic moment of the unpaired electron spins in the paramagnetic ion is not spherical in symmetry, the dipole–dipole interaction between the electron's magnetic moment and the nuclear magnetic moment does not average to zero. This gives rise to the so-called dipolar terms, σ_d. For axial symmetry σ_d is given by:

$$\sigma_d = \frac{H - H_0}{H_0} = -G(\chi_{\parallel} - \chi_{\perp}) \tag{3}$$

where G is a geometric factor $(3\cos^2\theta - 1)/R^3$, $\chi_{\parallel}$ is the atomic susceptibility in the direction of the axis of symmetry, R is the distance between the metal ion and the nucleus, and θ is the angle between R and the symmetry axis. Eq. (3) is derived under the assumption that $\langle r^{-3} \rangle$ for the unpaired electron orbitals is much larger than R^{-3}. If the ground state is a simple S state with no orbital degeneracy and any zero field splitting less than kT, $\chi_{\parallel}$ can be written as $g_{\parallel}^2 \beta^2 S(S+1)/3kT$, etc. For lower symmetries an additional geometric term is added to Eq. (3). This 'metal centered' pseudocontact shift depends on molecular geometry and will disappear in molecular systems in which the site symmetry at the metal ion is one of the higher symmetries having more than one symmetry axis greater than C_2 [15].

Kurland and McGarvey [18] have shown that it is possible to have a sizeable pseudocontact contribution even for systems of high symmetry if appreciable unpaired spin is transferred into p and d orbitals of ligand atoms. This 'ligand centered pseudocontact contribution' occurs in systems of high symmetry only when there is π bonding with the metal ion and the degenerate ground state manifold is split by a spin–orbit interaction. This contribution can occur in any low symmetry system in which there is an appreciable density of spin in the ligand p or d orbital. It is proportional to the admixture of the ligand orbital and $\langle r^{-3} \rangle$ where r is the distance of electron in the p or d orbital and the nuclear spin. When present this contribution can be comparable to the metal ligand contribution because the larger value of $\langle r^{-3} \rangle$ compared to R^{-3} compensates for the smaller density of spin.

For lanthanide and actinide ions, the small crystal field splitting of the ground J state results in nearly equal population of all states which in turn produces a nearly isotropic magnetic susceptibility. In this case Bleaney [19] has shown that even though the T^{-1} contribution is zero there is a sizeable T^{-2} contribution to the metal ligand dipolar shift. In this case the contribution is proportional to the same geometric factors but the other factor depends on crystal field parameters, g_J, and $J(J+1)(2J+3)(2J-1)$.

It has been proposed for the lanthanides that the contact and dipolar contributions could be separated on the basis of temperature dependence since the contact contribution has a T^{-1} term while the dipolar term is T^{-2}. This is doomed to failure for both experimental and theoretical reasons. Experimentally, the range of experimental temperatures is not sufficient to make a good separation due to the inaccuracy of the assumed value for H_0. Theoretically, it is known that the contact term is not truly a Curie Law dependence [20]. Recent data on NMR of paramagnetic molecules may be found in a review [21].

2.3. EPR and unpaired spin delocalization

The presence of unpaired spin in reduced species of HPA gives rise to an EPR spectrum whose pattern depends considerably on the number of atoms acquiring the unpaired electron and the temperature. For axial MO_6 complexes to which the reduced form of HPA containing V^{4+}, Mo^{5+} or W^{5+} belong, the EPR spectrum usually has an anisotropic pattern at low temperatures and may be described by the following spin Hamiltonian [22]:

$$\mathcal{H} = g_{\|}\beta H_z S_z + g_{\perp}\beta(H_x S_x + H_y S_y) + A_{\|} S_z I_z + A_{\perp}(S_x I_x + S_y I_y) \quad (4)$$

where S is the electronic spin, I is the nuclear spin, and A is the hyperfine splitting constant. Using the EPR parameters and data from the optical spectra, the atomic orbital coefficients in the corresponding MO and the degree of covalency or the electron density transfer may be estimated.

At elevated temperatures the EPR spectrum becomes isotropic due to molecular tumbling and to electron delocalization over several atoms. In a study of the temperature dependence of the EPR line width the electron hopping rate may be

evaluated [23–26]. However, the isotropic interaction of the electron with many atoms in the polymetalate sphere does not usually result in a resolved spectrum. Only interaction of a single electron with two or three vanadium atoms in mixed anions has been observed at room temperature (r.t.) and shows quite an effective hopping process [27–31].

The multiplicity of possible delocalization mechanisms of the unpaired electron density onto different nearest ligand atoms and moreover onto more distant ones makes it very difficult to give a quantitative description of the spin distribution. Most papers deal with the unpaired spin density distribution in 'central atom–organic molecule' systems which contain mainly carbon atoms involving only their p- and s-orbitals [21,32].

The most distinct feature of a polyoxoanion acting as a ligand is the alternating M–O bonds with different degree of participation of the oxygen orbitals in bonding both with the central and addenda atoms of the coordination sphere. Thus it is necessary to consider available data for the NMR chemical shifts of nuclei other than proton and carbon to discuss possible spin transfer mechanisms within a molecule and to stimulate interest in the spin distribution in large inorganic anions. Moreover comparison of NMR data for different nuclei of the same molecule may help in elucidation of the spin density distribution by σ- and π-mechanisms within the metal–oxygen framework. In some cases the observed chemical shifts may be compared with EPR parameters and nuclear–nuclear coupling observed in NMR spectra.

When only the nucleus of HPA is considered the electron density distribution might be well described but when the NMR of other nuclei is considered, some questions arise which require a more complex approach. Here we shall consider NMR and EPR data beginning with polyoxoanions where the central atom is loosely bound to oxygen and hence only weak X···O···M bonding exists.

3. Heteropolyanions with paramagnetic central atoms

3.1. f-Electrons in $XO_{12}Mo_{12}O_{30}^{8-}$

In most symmetrical HPA $XO_{12}Mo_{12}O_{30}^{8-}$ (symmetry T_h) a heteroatom X^{4+} (Ce, Th, U, and actinides) [33,34] is in the center of practically regular icosahedron formed by the O_a atoms. The structure and its fragment are given in Fig. 1. The completely resolved ^{17}O-NMR spectra of the two HPA reveal the three expected lines [35,36] (Table 1), which can easily be attributed to three types of oxygen atoms (see stick diagram).

Despite the paramagnetism of U($5f^2$), the ^{17}O-NMR spectra for both anions are remarkably similar. The resonance line corresponding to O_c with the lowest δ is pH-sensitive and shifts to higher values with neutralization, showing the strong shielding of these oxygen atoms upon protonation.

The negative shift (-10 ppm) of the O_a line (not shifted upon protonation or deprotonation of O_c) assigned to oxygen atoms forming an icosahedron around the

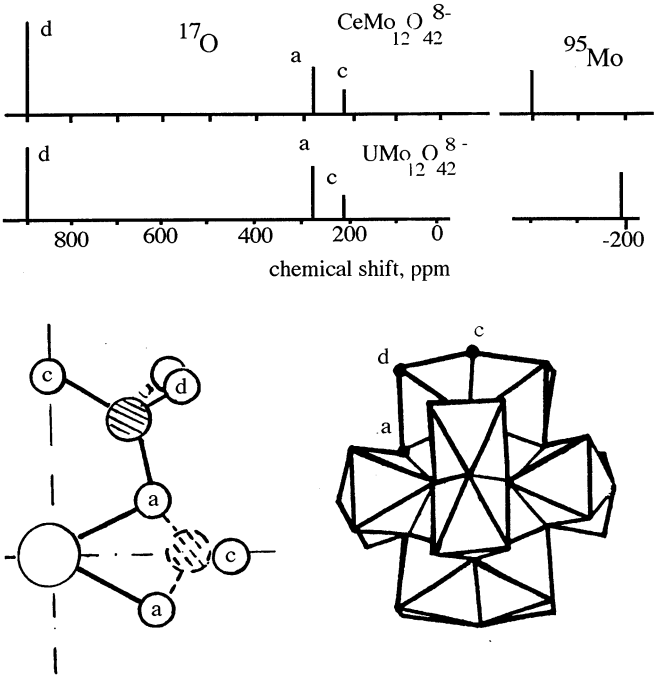

Fig. 1. The structure and the fragment of $XMo_{12}O_{42}^{8-}$ and ^{17}O-NMR shift diagram.

uranium atom, may reflect both the slight changes in the geometry of the whole HPA [33,34] and the influence of the U($5f^2$) electrons. The oxygen atoms O_a forming the polyhedron around the U^{+4} ion have sp^3 hybridization and present only a σ-pathway for delocalization of spin density. There is no possible π-route to transfer electron density and only spin transfer through σ-bonds may be proposed to produce the negative shift of O_a oxygen atoms. The small magnitude of this shift compared to the substantial shielding observed for Mo is striking and needs an explanation. The high point symmetry for the uranium ion site rules out any pseudocontact contribution, and the small shifts for the oxygen atoms rules out any ligand centered pseudocontact contributions. It is possible that for the O_a atoms, the covalent and polarization mechanisms cancel each other but the same is not true for Mo since different MOs contribute to each mechanism. A large shift for

Table 1
The ^{17}O- and ^{95}Mo-NMR chemical shifts[a] for HPA $XMo_{12}O_{42}^{8-}$ [35,36]

Anion	O_a	O_b	O_c	Mo
$CeMo_{12}O_{42}^{8-}$	284	215	898	0
$UMo_{12}O_{42}^{8-}$	274	193	900	−192

[a] Measured relative to $H_2^{17}O$ and $Na_2^{95}MoO_4$ at in aqueous solutions.

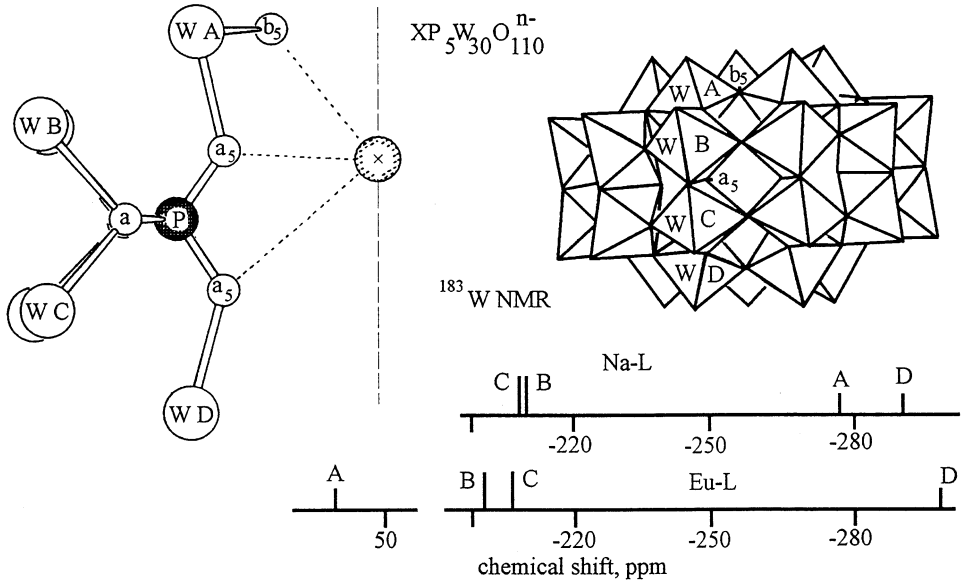

Fig. 2. The structure and fragment of $XP_5W_{30}O_{110}^{n-}$ and ^{183}W-NMR chemical shift diagram.

another metal atom with a small shift for the bridging atom to the paramagnetic site is not a unique phenomenon as we shall see further along.

3.2. *f*-Electrons in $XP_5W_{30}O_{110}^{(15-n)-}$

The quite unique HPA $XP_5W_{30}O_{110}^{(15-n)-}$ may serve as a bridge for the gap between the 3D-extended oxide structures and conventional metal complexes due to mostly vertex shared WO_6 octahedra forming a large curved surface. The crystal structure determination along with the ^{183}W-, ^{31}P-, and ^{23}Na-NMR have revealed [37] that this large anion is built up of five fragments of the Keggin structure as shown in Fig. 2. The interior sodium disturbs the original D_{5h} symmetry because it is located in one of the two pentagonal planes formed by the O_a atoms. The asymmetric upper and lower parts of the anion give rise to a four line pattern in the ^{183}W-NMR spectrum.

The sodium cation may be replaced by Bi^{3+}, Ca^{2+}, U^{4+}, and some Ln ions. Paramagnetic substituents induce large paramagnetic shifts in the ^{31}P-NMR and these shifts will be discussed below. The $P_5W_{30}O_{110}^{(15-n)-}$ cage (denoted as L) does not allow any large cation to enter its cavity freely because of the small aperture formed by the corner bridging O_b atoms. The Na–O_a distance is 2.66 Å giving an apparent sodium ionic radius equal to 1.26 Å in a rather unusual coordination. This is a quite large radius when compared to the radii of Ce^{4+} or U^{4+} in the $XO_{12}Mo_{12}O_{30}^{8-}$ icosahedron (X – O_a is 2.52 Å) [33,34] or in the $XO_8W_{10}O_{30}$ square antiprism (2.38 Å for Ce^{4+}–O_a [38], 2.31 Å for U^{4+}–O_a [39], 2.43 Å for Er^{3+}–O_a [40]).

So far only the ^{31}P-NMR spectra have been recorded for many of the large number of complexes $LnL^{(15-n)-}$ with the paramagnetic Ln inducing large paramagnetic shifts ([41]a). As deduced from analysis of the observed δ, (excluding the Eu complexes) 75–94% of the phosphorous shift comes from the dipolar contribution. Thus some small amount of spin density is transferred by the O_a oxygens but the rather loose $Ln-O_a-P$ bonding prevents any sizable transfer.

Unfortunately ^{183}W-NMR spectra were measured only for the EuL^{12-} complex and for no other diamagnetic LnL^{12-}. However with some approximations we may use the chemical shifts for NaL^{14-} to estimate the dipolar contribution to the observed ^{183}W-NMR chemical shifts of the different W atoms.

Creaser et al. ([41]a) have calculated from the dependence between the ^{31}P-NMR chemical shifts and the Golding constant, $\langle S_z \rangle$, [17] (the averaged spin of the electronic configuration) that 44% of the shift (or +5 ppm) in the Eu*L*-complex is from the dipolar contribution. If the Eu^{3+} cation is assumed to be located in the sodium site (in the plane of the pentagon formed by O_a) the dipolar contributions for the ^{183}W-NMR shift are calculated to be as shown in Table 2. However, if the Eu^{3+} were to occupy a site between the pentagon O_a and the pentagon O_b, forming a distorted antiprism EuO_{10}, the estimated dipolar shifts would be those also shown in Table 2. These second set of calculated shifts are close to the experimental values for all ^{183}W-NMR shifts except W_a. We may therefore assume that the Ln occupy the site inside the LnO_{10} polyhedron, which seems more realistic (a reviewer has informed us of a recent structure determination ([41]b), which confirms this location for the Eu^{3+} ion).

Thus we see that only the W_a atoms experience a contribution from the 'contact' shift. The sign of the shift is opposite to that which would be predicted by the

Table 2
The ^{183}W- and ^{31}P-NMR chemical shifts[a] for $XP_5W_{30}O_{110}^{n-}$ ([37], [41]a)

X	^{31}P	X	^{31}P	X	^{31}P
Nd	−15.9	Dy	−68.1	Yb	9.1
Sm	−9.5	Ho	−40.0	Lu	−10.1
Eu	10.8	Er	1.8	U (IV)	−15.5
Tb	−27.2	Tm	17.6	Ce (IV)	−16.0

	W_a	W_b	W_c	W_d	P
Na^+	−277.3	−209.6	−211.6	−289.6	−10.1
Eu^{3+}	62.5	−201.7	−209.0	−297.6	0.7
$\Delta\delta$	339.8	7.9	2.1	−7.9	10.8
[b] G_{na} 10^{-3}	0.57	−2.77	−1.51	7.67	−14.5
$\Delta\delta_{dip}$(-D)	<0.1	1.0	0.5	−2.6	5.0
[c] G_{Eu} 10^{-3}	−19.0	−2.75	−0.29	4.25	−2.1
$\Delta\delta_{dip}$(-D)	45.0	6.0	0.7	−10.1	5.0

[a] Aqueous solution, shifts are relative $Na_2^{183}WO_4$ and $H_3^{31}PO_4$.
[b] *G* calculated from Na-position.
[c] *G* and $\Delta\delta_{dip}$ calculated for Eu displaced from Na position.

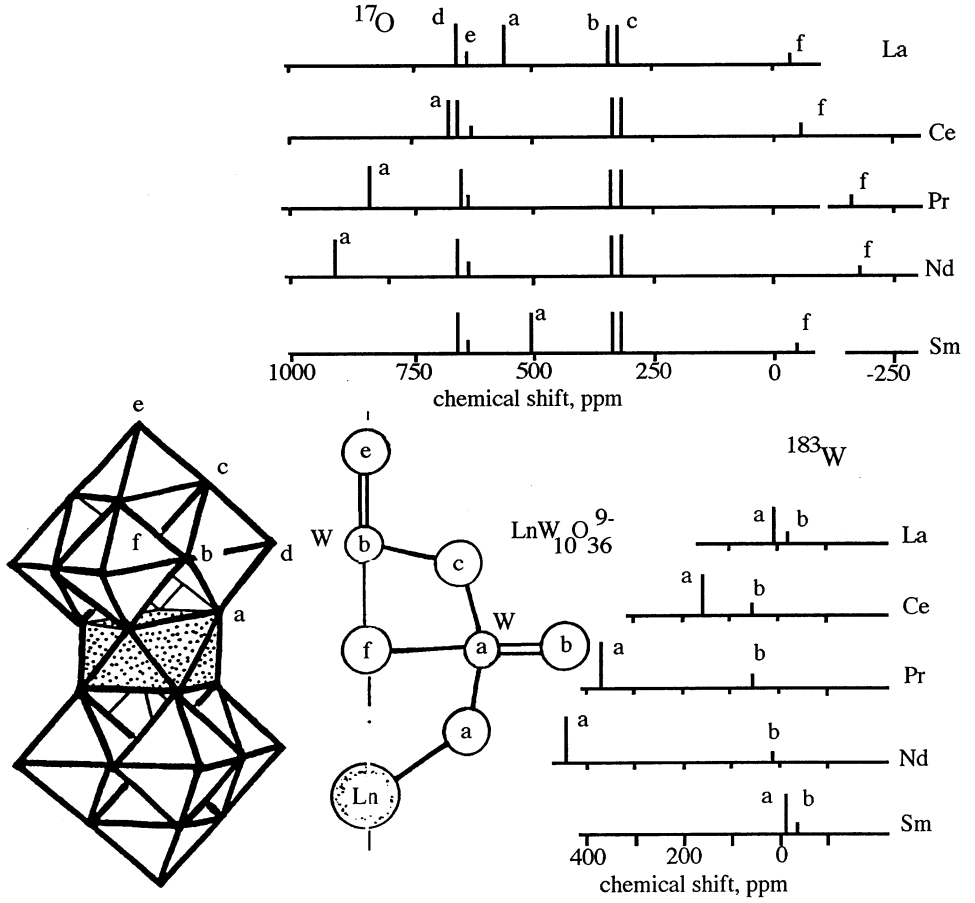

Fig. 3. The structure and fragment of $XW_{10}O_{36}^{n-}$ and ^{17}O- and ^{183}W-NMR chemical shift diagram.

polarization mechanism of spin transfer but is consistent with the covalent mechanism. The shifts are not as large as those observed for the W_1 and W_2 atoms in $Eu(lig)_2$ (see Table 5).

The measurement of the ^{17}O-NMR would be beneficial to elucidate both the location of Ln and the detailed mechanism of the spin distribution. The four electrons are assumed to be delocalized in the reduced form of this quite interesting polyanion [37].

3.3. *f*-Electrons in $XO_8W_{10}O_{28}^{n-}$

There is another paramagnetic system involving lanthanides and actinides as heteroatoms (X), which is fairly fixed: $XO_8W_{10}O_{28}^{n-}$. These HPA are formed by two former highly symmetric anions $W_6O_{19}^{2-}$ with one $W{=}O_d$ group removed from each

For many of these complexes both the ^{17}O- and ^{187}W-NMR spectra have been reported [42–46] and the observed lines may be assigned by the peak intensity ratios and from the general parallelism between the chemical shifts of the two nuclei, with the larger δ for the ^{17}O corresponding to a larger δ for ^{183}W in the same WO_6 octahedron in a polyoxoanion. The shifts of some lines in the diamagnetic complexes may reflect changes in bond lengths as observed in the vibrational spectra of a series of complexes [47].

For the oxygen atoms, only the O_a and O_f atoms have shifts that appear to involve spin transfer. The small shifts for O_b, O_c, O_d, and O_e follow the characteristic sign changes associated with the dipolar shift equation of Bleaney [19], particularly the characteristic change in sign between Ho^{3+} and Er^{3+}. The large shifts in O_a are positive in the first half of the period and negative in the second half, which is characteristic of the polarization mechanism or the covalent mechanism involving π transfer. Since the oxygen atoms in the bridge $X–O_a–W_a$ are in the sp^2 hybridization, π spin transfer is possible. The correlation of the shifts with the Golding constant, $\langle S_z \rangle$ would support either mechanism. The smaller magnitude shifts observed for O_f are all negative which is consistent only with covalent spin transfer by σ bonds but there is no direct pathway to transfer the spin density this way (the distance $Ln–O_f$ is too large), so the transfer must come from the four W_a atoms.

The signs for the NMR shifts in W_a are also consistent with the polarization mechanism or covalent spin transfer through the π orbitals as was the case for O_a atoms. The shifts for W_b are mostly dipolar but the lack of a sign reversal between Ho^{3+} and Er^{3+} indicates a small negative contact shift, while the positive shifts observed in the first half of the periodic series are too large to be accounted for by the dipolar shift. Thus the small contact shift for this atom is also consistent with either the polarization mechanism or covalent transfer via the π system.

The larger participation of the U5f orbitals in the electron transmission into the W5d orbitals is clearly indicated from the shifts for $UW_{10}O_{36}^{8-}$ (Table 3). The ^{183}W shifts are much larger than that observed for $PrW_{10}O_{36}^{9-}$, the electronic analog of the U complex, while the ^{17}O shift for the nearest O_a oxygens are almost the same. It is of interest to note that there is a substantial spin transfer to W_b even though the bridging oxygen in $W_a–O–W_b$ does not experience any spin density. A similar behavior was observed for $UO_{12}Mo_{12}O_{30}^{8-}$.

3.4. d^6 and d^7 electrons in tetrahedral $CoO_4W_{12}O_{36}^{n-}$

A large family of HPA are formed with the Keggin structure by tungsten where the heteroatom occupies the tetrahedron formed by the internal O_a atoms. A number of such HPA can be formed with d-metal cations. For example, the Co^{2+} ion may occupy the cavity of the Keggin anion retaining, according to X-ray structural data [48], the regular tetrahedral configuration (Fig. 4).

Co^{2+} can be reversibly oxidized, keeping the same structure. However, due to the electronic configuration E, the tetrahedron $Co^{3+}O_4$ undergoes the Jahn–Teller distortion, being elongated along the C_2 axis [49].

The ^{17}O-NMR spectrum of $Co^{2+}O_4W_{12}O_{36}^{6-}$ reveals three of the expected four lines, the fourth line due to O_a is not observed due to line broadening [50]. The diamagnetic analog $H_2O_4W_{12}O_{36}^{6-}$ displays four lines in the intensity ratio 12:12:12:4 (Table 4). The paramagnetism of the Co^{2+} ion shifts the NMR lines of the oxygen atoms relative to those in the diamagnetic analog. All three lines for the Co^{2+} complex show the expected paramagnetic shift temperature dependence. The temperature dependence is not strictly T^{-1} and therefore a linear plot of δ vs. T^{-1} does not extrapolate to the diamagnetic analog, but close enough to assign the resonances. The line widths also support the assignment.

Attempts to fit the data to Eq. (5)

$$\delta = aT^{-1} + bT^{-2} \tag{5}$$

in order to separate the Fermi contact from the pseudocontact shift were unsuccessful due to an inadequate temperature interval. It is now known [16,51] that for Co^{2+}, in tetrahedral coordination, the temperature dependence in Eq. (5) is entirely inadequate for representing the temperature dependence of the paramagnetic shift and that such attempts to make a separation based on temperature dependence are meaningless. Acerete et al. [52] attempted a similar analysis for the ^{183}W resonance and claimed it showed the pseudocontact (ligand centered) contribution to dominate the shift. The problem should probably be reexamined.

The equivalence of all the tungsten atoms in the isotropic system is confirmed by the presence of a single line in the ^{183}W-NMR which is shifted to high field with $\delta = -915$ ppm [50,52]. There should be no metal centered dipole contribution to this shift due to the T_d symmetry at the Co^{2+} site.

Table 3
The ^{17}O- and ^{183}W-NMR chemical shifts[a] for $XW_{10}O_{36}^{n-}$ [43,45]

X	O_d	O_e	O_a	O_c	O_b	O_f	W_a	W_b
La	656	637	559	340	326	−34	1.5	−19.2
Ce	652	627	670	337	313	−60	155	51
Pr	649	634	844	338	317	−162	378	53
Nd	652	632	910	337	315	−179	444	17
Sm	657	638	508	339	321	−48	−10	−31
Eu	667	652	138	349	340	−94	−611	−18
Gd	643				345	306		−108
Tb	621	559	−1340	200	178	−580	−1620	−188
Dy	629	92	−1100	269	235	−360	−1135	−132
Ho	627	593	−780	284	255	−221	−770	−119
Er	645	668	−580	394	385	−162	−372	−32
Yb							23.4	82.6
Y	655	640	538	345	323	−35	−11	−28
Th	675	655	546	355	337	−49	0.6	−11.9
U	650	650	878	359	330	−145	970	270

[a] Measured relative to $H_2^{17}O$ and $Na_2^{183}WO_4$, respectively, in aqueous solutions.

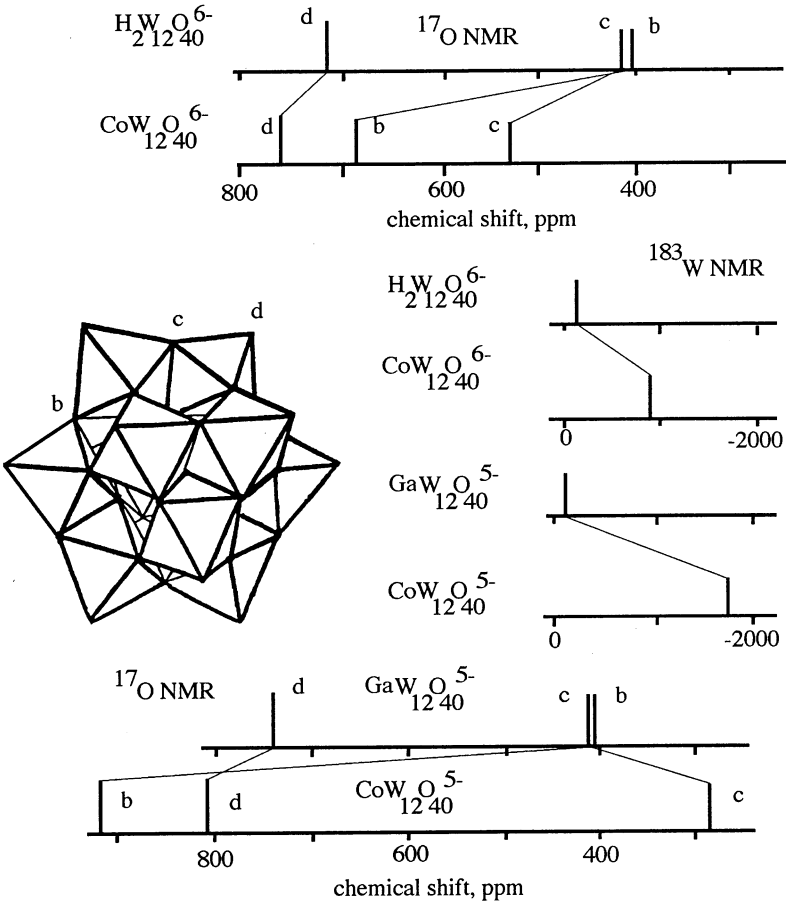

Fig. 4. The structure of $CoW_{12}O_{40}^{n-}$ and ^{17}O- and ^{183}W-NMR chemical shift diagram.

Since the p-orbitals of O_b and O_c do not mix with Co^{2+} 3d orbitals and there is no dipolar contribution from the d^7 electrons due to the symmetry, the isotropic shifts should be due solely to the interaction with the spin density in the W-or-

Table 4
The ^{17}O- and ^{183}W-NMR chemical shifts[a] for $XW_{12}O_{40}^{n-}$ [50]

X	O_b	O_c	O_d	W
Co(II)	694	526	759	−915
H_2(II)	410	414	722	−110
Co(III)	929	297	817	−1790
Ga(III)	410	417	756	−89

[a] Measured relative to $H_2^{17}O$ and $Na_2^{183}WO_4$, respectively, in aqueous solutions.

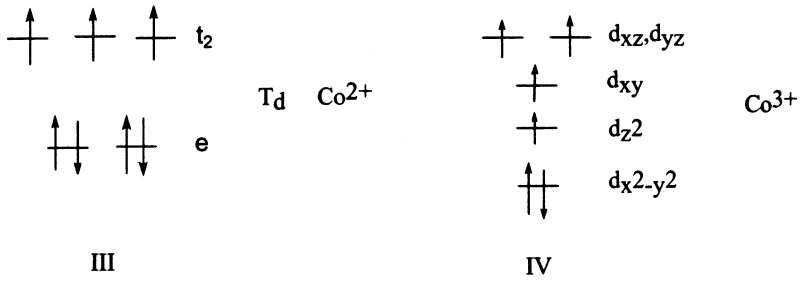

Scheme III and Scheme IV.

bital(s). Since the WO_6 is distorted there could still be a dipolar contribution from any spin in the d orbitals of the tungsten ion. According to our estimates (presented in Section 5.1), the dipolar contribution to the isotropic shifts of the terminal oxygen will be ca. -129 and $+45$ ppm for the bridging oxygen atoms if one d-electron were localized on the metal in the coordination sphere and its spin aligned with the W=O_d bond. The actual contribution is, of course, much smaller since if one electron were delocalized from the cobalt ion it would be shared by 12 tungsten atoms. It is more reasonable to estimate these dipolar shifts to be no more than a few ppm at best.

As shown in Scheme III, the three unpaired electrons are t_2 in the tetrahedral coordination. In tetrahedral coordination, however, both e and t_2 can be involved in σ and π bonding and the weak crystal field allows the Co^{2+} unpaired spins to occupy both types of orbitals. The unpaired spin transfer Co $\rightarrow$ W should occur through the O_a atoms each of which is bonded to three W atoms (sp^3 hybridization). Thus the spin density may be transferred into the p- and s-orbitals of O_b, O_c, O_d and from there to the tungsten atoms. Unfortunately, the resonance line for O_a was not visible and the nature of spin delocalization onto that oxygen atom is not known. The large up field shift for ^{183}W indicates a negative spin density on the tungsten atoms.

The chemical shifts relative to the diamagnetic analog $H_2O_4W_{12}O_{36}^{6-}$ demonstrate very different distributions of spin density, O_d has a shift of $+37$ ppm, O_b has shift of $+284$ ppm, and O_c has a shift of $+112$ ppm. Once again the large paramagnetic shift for O_b suggests a large π-contribution to the MO in the *xy* plane. The much smaller paramagnetic shift observed for O_d may be associated with the short W=O bond. Further calculations of the different contributions to the shift are very much needed.

The oxidation of Co^{2+} in the Keggin structure brings about an unusual tetrahedral oxygen coordination around the Co^{3+} ion. The $CoW_{12}O_{40}^{5-}$ gives a single line in the ^{183}W-NMR spectrum, substantially shifted to high field showing all tungsten ions to be equivalent [50,52]. At the same time three lines are observed in the ^{17}O-NMR spectrum (Fig. 4, Table 4) [50]. The negative shift of the line assigned to O_c is puzzling and different from what was found for the Co^{2+} analog.

As might be expected, the CoO_4 tetrahedron in the crystalline state was found to have undergone a tetragonal distortion along the C_2 axis giving two different edges O_a–O_a equal to 2.7 and 3.5 Å, respectively [49] and a slight splitting of the e and t_2 orbitals, as shown in Scheme IV, could be predicted. This distortion should carry over to the whole framework of the $W_{12}O_{36}$ ligand. This distortion should result in non-equivalence in different sets of oxygen and tungsten atoms and, therefore, several lines should be seen in the ^{17}O- and ^{183}W-NMR spectra. However, very simple spectra typical of an undistorted system are observed. It has been proposed [50] that in solution, this is due to a dynamic Jahn–Teller distortion which would average the tungsten resonances and give rise to only three oxygen resonances (Fig. 4).

Acerate et al. [52] has estimated the dipolar contributions to the ^{183}W shift using Eq. (3) but the values are surprisingly 100 times larger than those estimated for the Co^{2+} complex. Inspection of the equations given in the paper [52] reveals that the contribution should be two orders of magnitude less.

The unpaired electron in the Co d_{z^2} orbital probably induces the spin density in the W $5d_{xy}$ orbital, which in turn distributes it into the p-orbitals of the bridging oxygen atoms. The dipolar contribution to the ^{17}O-NMR shifts for O_d and $O_{b,c}$ from spin density in W will not exceed -10 to $+3$ ppm, respectively, if one electron were to be delocalized into the tungsten–oxygen framework. The difference, however, between the paramagnetic shifts for O_b and O_c is quite large (639 ppm) and greatly exceeds the $\Delta\delta$ observed for the bridging oxygens. Moreover, the signs of the isotropic shifts for these two oxygens are opposite in sign. Several approaches can be suggested to explain such differences.

(a) In the dynamic situation, when the tetrahedron CoO_4 is 'breathing', the nearest bridging oxygens O_b may interact directly with the Co d_{z^2} orbital (see Scheme IV) leaving no spin density for O_c.

(b) We might suppose that the tetrahedron CoO_4 maintains its distortion but rotates inside the tungsten–oxygen cage. If the S_4 axis is chosen as the principal one, the rotation will replace O_b for O_c and vice versa, forming two rotation cones with different angles relative to S_4 with angles of 30 and 70°, respectively. The $CoO_{b,c}$ distances are 3.69 ± 0.29 Å (atomic coordinates [48]). At the same time, the terminal oxygens O_d and bridging oxygens will occupy positions that have been proposed for the so-called 'pseudo-Keggin structure' [53,54] corresponding with $m3m$ symmetry. Anions of this type in crystals were reasonably explained by a statistical disordering of HPA, resulting in the positional averaging of the bridging atoms [55]. This rotation will also average the bridging atoms.

This situation in solution is not abnormal. The dynamic averaging of five tungsten atoms in HPA $P_2W_5O_{23}^{n-}$ with dissimilar tungsten atoms has been observed and was explained by the rotation of PO_4 tetrahedra [56]. A rapid inversion of PO_4 is found in the transformation of A–PW_9O_{34} into B–PW_9O_{34} including a similar rearrangement of the bridging oxygen atoms [57]. Finally, the transformation of $Mo_7O_{24}^{6-}$ in solution without the intervention of the solvent molecules has been observed recently [58].

The two different angles would result in different signs for the dipolar shift (see Eq. (3)). If we assume the contact shift is the same for the two sites and knowing the geometric factors, we can use the two shifts to estimates the contact and dipolar shifts for the two oxygens. We obtain $\delta_c = 328$ ppm, $\delta_{dip} = 128$ and -508 ppm. This large δ_c is expected but the dipolar contribution is too large to be realistic.

(c) A third, more reasonable answer, which does not involve a large dipolar shift, can be proposed. The dynamic distortion may cause the oscillation or delocalization of the spin density through the bonds. Such a transfer of the spin density involves only the O_b oxygens by the formation of cycles as shown in Schemes V and VI.

The spin density circulation would induce by a direct mechanism, a positive shift for O_b and by an indirect mechanism a negative shift for O_c. The situation is similar to that of the circulation of a polaron and a spin polaron which is considered in Section 5. The possibility of the transfer of the e_g spin paired electrons cannot be excluded, and this will be discussed later.

4. Paramagnetic cation and HPA as inorganic macroligands

4.1. Lacunary HPA as a ligand

As soon as the HPA of the Keggin anions, $XO_4W_{12}O_{36}^{n-}$, and the Dawson anions, $(XO_4)_2W_{18}O_{54}^{6-}$, with one W=$O_d$ group removed became available in rather pure form, many papers appeared devoted to the preparation of related complexes [3,5]. A large dipolar contribution to the isotropic shifts from a paramagnetic ion is assured in the lower symmetry of these complexes. The lacunary anions $XW_{11}O_{39}^{n-}$ (lig) (Fig. 5) and $P_2W_{17}O_{61}^{10-}$ (LIG) (Fig. 5) with four or five oxygen donor atoms form fairly stable complexes with d-, p-, or f-cations [59,60].

The size of the lanthanide cations is too large to enter the octahedral cavity of the lacunary HPA so the cation stays on the four surface oxygen atoms which form after the removal of the W=O_d group [60–65]. The ^{183}W-NMR spectra for $Ln(lig)_2$ and $Ln(LIG)_2$ complexes enables us to establish the different geometric forms of the

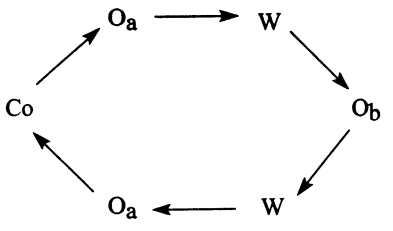

V

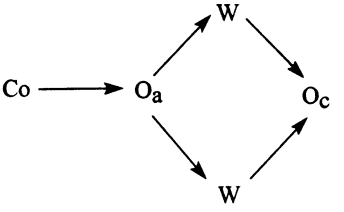

VI

Scheme V.

Scheme VI.

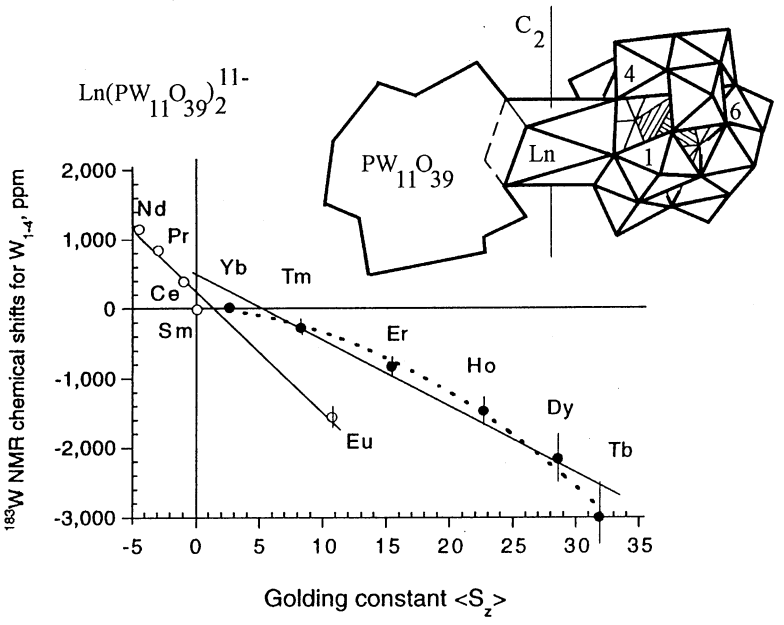

Fig. 5. The structure of $Ln(PW_{11}O_{39})_2^{n-}$ and the plot of the average of the four ^{183}W-NMR chemical shifts from the closest tungstens versus Golding [17] $\langle S_z \rangle$ for the Ln ion.

complexes in solution. The ^{183}W-NMR on $Ln(lig)_2$ consists of six lines for the light lanthanides indicating a complex with a symmetry plane, while the heavier lanthanides with a larger number of ^{183}W-NMR lines must form dissymmetric conformations. The ^{31}P-, ^{17}O-, and ^{183}W-NMR shifts are listed in Table 5 and the ^{183}W shifts [61,62] for $^{183}W_1$ and $^{183}W_4$, the closest to the Ln atoms, are plotted against the Golding parameter, $\langle S_z \rangle$, in Fig. 5. The shifts for $^{183}W_{2,3,6}$ and ^{31}P obey the sign alterations of the Bleaney equation [19] and are therefore dipolar in origin. The near linearity of the plots of $^{183}W_{1,4}$ against $\langle S_z \rangle$ indicates a polarisation mechanism of spin transfer for these metal atoms, but the hyperfine interaction is stronger for the lighter lanthanide complexes.

The ^{17}O shifts for Ln–O–W appear to be a mixture of dipolar and contact shifts while those observed for O=W and W–O–W sites are too small and random to make any assignment.

The situation is drastically changed when a paramagnetic d-cation is introduced into the lacunary $XO_4W_{11}O_{35}^{n-}$, with M^{m+} placed into the octahedral cavity. Very large isotropic shifts were observed in both the ^{31}P- and ^{183}W-NMR spectra [14,66,67] and sometimes for ^{17}O-NMR [66,67]. NMR data for Co^{2+}, Ni^{2+}, Ru^{2+}, Ru^{3+}, Fe^{3+}, and Cr^{3+} complexes are given in Table 6, together with the chemical shifts for the diamagnetic Zn-analogue [69]. The unambiguous assignment of the lines in the Zn-analogue were done using the $^2J_{W-W}$ connectivity pattern [14].

Table 5
The ^{31}P-, ^{183}W-, and ^{17}O-NMR chemical shifts[a] for Ln(lig)$_2$ [63,64]

Ln	P	W ($-\delta$)				O_d				$O_{b,c}$ (Ln–O–W)			
La	−11.9	144	130	150		708	685	670		432	386	360	
		128	104	117							(632, 614)		
Ce	−19.3	−325	−181	141		711	686	669		430	385	355	
		118	96	113							(782, 737)		
Pr	−14.6	−829	−547	133		711	688	677		430	389	356	
		114	93	113							(1000, 916)		
Nd	−24.2	−1027	−999	131		713	688	677		430	387	356	
		115	94	113							(1084, 988)		
Sm	−15.4	159	140	148		710	688			422	388	356	
		125	103	116							(514, 558)		
Eu	−1.2	1761	1635	179		708	689			410	387	359	
		136	119	124							(655, 632)		
Gd	–	248	170			710	689			383	372	355	
		152	154										
Tb	−223	3604	3318	2842	2779	723	710	683	672	413	381	357	
		290	277	203	206								
		164	167	188									
Dy	−108	2657	2429	2141	2029	711	687	679		401	372	352	
		246	240	172	164								
		138	161										
Ho	−109	1830	1681	1572	1427	710	792	685	678	396	380	373	355
		213	225	159	163						(443, 427)		
		131	135	154									
Er	61.4	1124	1007	905	887	712	687	675		398	378	352	
		157	163	114	119						(604, 641)		
		103	116										
Tm	217	484	407	420	408	717	708	684	670	400	391	360	
		102	103	82	89						(616)		
		72	77	80									
Yb	32	151	140	136	132	711	695			394	352		
		122	122	112	114								
		94	101	122									
Lu		159	184	135	133								
		144	146	123	124								
		102	104	115									

[a] Measured relative to $H_3^{31}PO_4$, $H_2^{17}O$ and $Na_2^{183}WO_4$, respectively, in aqueous solution at 323 K.

Some insight into the nature of the paramagnetic shifts may be obtained from the data for those Dawson complexes, in which one tungsten is replaced with a paramagnetic centre resulting in the two halves becoming unequal. The NMR data for ^{31}P in these complexes is given in Table 7. P_a is in the half containing the paramagnetic centre and P_b is in the other half. In the case of transition complexes the unpaired electrons can occupy both d_σ and d_π orbitals, which can form chemical bonds with W 5d orbitals through the σ and π orbitals of the bridging oxygen atoms.

In the α_2-$P_2W_{17}Mo^{V}O_{62}^{8-}$ (Fig. 7), molybdenum is located in the cap triplet group giving rise to the positive ^{31}P shift for P_a atoms connected to Mo^{V} by the O_a atoms, while the second P_b atom in the unperturbed half of the anion exhibits a negative shift of $\Delta\delta = -1.1$ ppm [70]. Electron density transfer through the rather long chain involving the long W_5–O_a–P_b bond seems unlikely and it may be assumed that P_b experiences only a dipolar interaction. Using the structural data [71,72] the dipolar term for P_b is calculated to be $-$ 23.5 ppm, giving $\delta^c = +18.7$ ppm. This contact shift is due to the spin polarisation mechanism because the d_{xy} orbital is orthogonal to the corresponding O_a–Mo bond making covalent transfer difficult. This calculation of the contact shift should have been made using the chemical shift of P_a in a similar ion containing a diamagnetic metal ion of the same charge, but it is believed that this chemical shift is small in this case.

It is worth noting that in α-$P_2W_{17}Mo^{V}O_{62}^{7-}$, when Mo^{V} occupies the belt position, the resonance line for P_b is positively shifted [70]. This may result from both a partial indirect transfer through the bonds and from a dipole term in which $(\chi_\parallel - \chi_\perp)$ in G of Eq. (3) is greater than zero [26].

Quite large ^{31}P-NMR shifts have been observed for Co^{II} and Ni^{II} complexes which have unpaired electrons in the e_g orbitals of the metal ion that interact in a σ fashion with the P–O_a bond [14]. Due to the similarity in the position of the Co and Ni ions in both the Keggin anion and in the α_2-Dawson anions, we can use the data for the latter to estimate the dipolar contribution in the former. It can be

Table 6
The ^{183}W- and ^{31}P-NMR chemical shifts[a] for $PW_{11}MO_{39}^{n-}$ and $SiW_{11}MO_{39}^{n-}$

XM	W_1	W_4	W	W*	W	W	P	Ref.
PZn^{II}	−73	−157	−107	−130	−131	−140	−11.5	[14]
PCo^{II}	–	–	−192	−256	725	818	458	[14]
PNi^{II}	–	–	−121	−197	593	642	472	[14]
PRu^{III}	–	–	−112	−200	−146	−560	−87	[68]
PFe^{III}	–	–	−151	−139	64	76	14	[66]
PCr^{III}	−211	−285	118	−85	−137	−152	−3.5	[67]
$SiCo^{II}$	–	–	−222	−280	438	390		[14]
$SiNi^{II}$	–	–	−134	−225	328	308		[14]
PRu^{II}	159	292	−89	−102	−111	−136	−8.7	[68]
PMo(NO)	20	39	−84	−96	−90	−101	−13.3	[69]

[a] Measured relative to $H_2^{17}O$ and $Na_2^{183}WO_4$, respectively, in aqueous solution at 330 K (W* peak intensity 0.5, the rest peaks with intensity of 1).

Table 7
The ^{31}P-NMR chemical shifts[a] in polyoxodiphosphates

	Anion	P		Ref.
1	$P_2Mo_{18}O_{62}^{6-}$	−2.8 (0.1*)		[123]
	$P_2Mo_{18}O_{62}^{7-}$ (1e)	(13.4*)		[124]
	$P_2Mo_{18}O_{62}^{8-}$ (2e)	−4.6 (−1.9*)		
	$P_2W_{18}O_{62}^{6-}$	−12.7		[70]
	$P_2W_{18}O_{62}^{7-}$ (1e)	−12.0		
	$P_2W_{18}O_{62}^{8-}$ (2e)	−0.4		
2	$P_2O_7Mo_{18}O_{54}^{4-}$	−21.7*		[133]
	$P_2O_7Mo_{18}O_{54}^{5-}$ (1e)	−22.8*		
	$P_2O_7Mo_{18}O_{54}^{6-}$ (2e)	−23.1*		
	Lacunary anions	P_a	P_b	
3	α_2-$P_2W_{17}MoO_{62}^{6-}$	−11.5	−12.3	[70]
	α_2-$P_2W_{17}Mo^{V}O_{62}^{7-}$	−3.8	−13.4	
	α_2-$P_2W_{17}VO_{62}^{7-}$	−10.8	−12.9	
4	α_1-$P_2W_{17}MoO_{62}^{6-}$	−11.4	−12.3	[70]
	α_1-$P_2W_{17}Mo^{V}O_{62}^{7-}$	−6.3	−9.2	
5	α_2-$P_2W_{15}Mo_3O_{62}^{6-}$	−10.4	−12.9	[70]
	α_2-$P_2W_{15}Mo_2Mo^{V}O_{62}^{7-}$	4.5	−13.5	
6	α_2-$P_2W_{17}ZnO_{61}^{8-}$	−8.0	−13.5	[14]
	α_2-$P_2W_{17}Co^{II}O_{61}^{8-}$	250	−23.7	
	α_2-$P_2W_{17}Ni^{II}O_{61}^{8-}$	228	−14.0	
	α_2-$P_2W_{17}Mn^{III}O_{61}^{7-}$	575	−12.5	
7	α_1-$P_2W_{17}ZnO_{61}^{8-}$	−7.9	−12.8	[14]
	α_1-$P_2W_{17}Co^{II}O_{61}^{8-}$	1135	−34.5	
	α_1-$P_2W_{17}No^{II}O_{61}^{8-}$	895	−16.6	
	α_1-$P_2W_{17}Mn^{III}O_{61}^{7-}$	700	8.0	
8	$[(\alpha_2\text{-}P_2W_{17}O_{61})_2Dy]^{17-}$	−95.1	−21.7	[46,62]
	$[(\alpha_2\text{-}P_2W_{17}O_{61})_2Ho]^{17-}$	−92.6	−21.4	
	$[\alpha_2\text{-}P_2W_{17}O_{61})_2Eu]^{17-}$	3.14	−13.23	
	$[(\alpha_2\text{-}P_2W_{17}O_{61})_2Yb]^{17-}$	−8.7	−22.76	
	$[(\alpha_2\text{-}P_2W_{17}O_{61})_2La]^{17-}$	−8.17	−14.15	
	$[(\alpha_2P_2W_{17}O_{61})_2Ce^{III}]^{17-}$	−14.0	−14.0	
	$[(\alpha_2\text{-}P_2W_{17}O_{61})_2Ce^{IV}]^{16-}$	−8.6	−13.6	
	$[(\alpha_2\text{-}P_2W_{17}O_{61})_2U^{IV}]^{16-}$	10.3	−10.1	
	$[(\alpha_2\text{-}P_2W_{17}O_{61})_2Th]^{16-}$	−8.3	−13.6	

[a] Measured relative to $H_3^{31}PO_4$ in aqueous solutions except those marked * measured in CD_3CN. P_a is bonded to the introduced cation through O_a.

assumed that the P_b atom experiences only a dipolar shift and this is confirmed by the nearly unchanged position of the P_b line in α_2-$P_2W_{17}NiO_{62}H_2^{8-}$ and by the analysis of ^{1}H- and ^{13}C-NMR in organic nitrogen bases in $SiW_{11}NiO_{39}$ [73]. The difference between the calculated dipolar shift and the observed shift gives a δ^c of 397 ppm for P_a in α_2-$P_2W_{17}CoO_{52}H_2^{8-}$. The ratio between this value and the corresponding δ_{obs} for the Ni complex is close to the ratio $S_{Co}(S_{Co}+1)/S_{Ni}(S_{Ni}+1)$ which indicates that a similar amount of spin density is transferred from both metal ions to P_a.

Much larger shifts for the P_a atom in the α_1-isomers demonstrate the greater ability of the O_a atom to to transfer spin density, presumably because it binds only two rather than three tungsten atoms to the phosphorous.

The assignment of the lines in the ^{183}W-NMR spectra is mostly speculative except for the line with an intensity of one which has to belong to the unique tungsten opposite to the paramagnetic ion that has been inserted into the anion.

It is worth noting that a similar spin delocalization is observed for the complexes with Ni^{2+} and Co^{2+} cations despite the different distribution of d electrons (Schemes VII and VIII). Only a σ-delocalization can occur for nickel which has only e_g unpaired electrons while the presence of one t_{2g} unpaired spin in Co^{2+} allows for some π-delocalization. Several mechanisms have been advanced [15,74] to explain this similarity.

Except for W_6, the tungstens are not assigned. W_1 and W_4, the nearest to the paramagnetic ion, are presumably not observed due to large line widths. $W_{2,3}$ have been assigned the positive shifts based on speculative arguments. Surprisingly W_6 is the most shielded but σ spin density can come through two W_2 atoms.

The importance of the π-mechanism for spin transfer is revealed by the marked difference in the ^{183}W shifts for $SiW_{11}MO_{40}H_2^{6-}$ and $PW_{11}MO_{40}H_2^{5-}$ found by Jorris et al. [14] The smaller shift for the former is consistent with the lower degree of spin delocalization deduced from the analysis of EPR spectra of the corresponding reduced forms [25,26].

Some paramagnetic complexes with iron, manganese, chromium and ruthenium have been studied by NMR [14,66,68]. Although both ^{183}W- and ^{17}O-NMR spectra have been observed, the assignment of the lines is rather unreliable due to complex equilibria in the solutions under study. Fedotov et al. [66] observed the change in the spin density distribution in $PW_{11}Fe^{3+}O_{39}^{n+}$ in a solution due to pH, probably due to the formation of the dimeric complex with the bridging oxygen, $PW_{11}O_{39}Fe–O–FeO_{39}W_{11}P$.

The Ni^{2+} and Co^{2+} cations induce large isotropic shifts in the ^{31}P-NMR spectra. This could be attributed to direct σ-transfer through O_a from the e_g electrons. All of the other cations in Tables 6 and 7 have their unpaired electrons in t_{2g} orbitals.

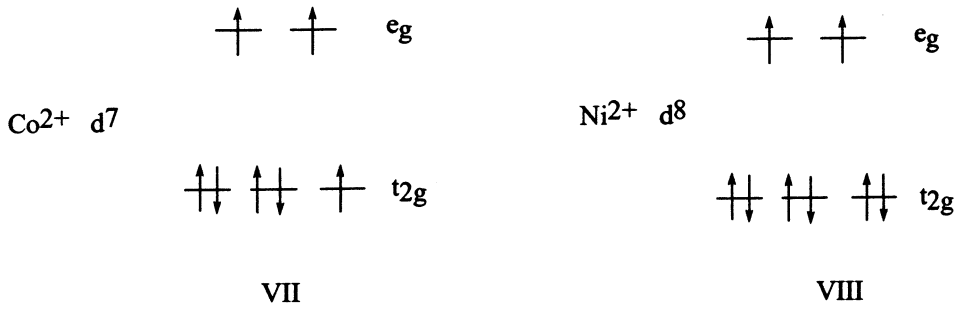

Scheme VII and Scheme VIII.

Low spin Fe^{3+} and Ru^{3+} have the unpaired electron in a t_{2g} orbital but the ^{31}P-NMR shifts are of opposite sign, perhaps due to different dipolar shifts. High spin Fe^{3+} results in a negative shift for both ^{31}P- and ^{183}W-NMR lines.

The rather unstable lacunary HPA, $PMo_{11}O_{39}^{7-}$, has a complex equilibrium in solutions with different M^{m+} ions but a marked positive shift in the ^{31}P-NMR line is induced by Co^{2+}. A possible elongation of the CuO_6 octahedron in $PMo_{11}CuO_{40}H_2^{5-}$ leaves the unpaired electron in a $3d_{x^2-y^2}$ orbital which is orthogonal to the P–O_a–Cu bond. The shifts due to d^1 and d^9 are different [65] but if the hole formalism is applied, the sign of the ^{31}P shift is understood. A similar negative shift is observed for ^{29}Si in $SiMo_{11}CuO_{39}$ [75].

4.2. Labile paramagnetic polycomplexes

The influence of a paramagnetic cation may be manifested not only in the inert, rather stable, complexes considered above. Some HPA such as the $XMo_{12}O_{42}^{8-}$ discussed in Section 3.1 (Fig. 1) can act as a macroligand using surface oxygens as donor atoms. This tridentate (or hexadentate in the presence of two cations) ligand may form complexes with cations of the d- and f-elements. The single crystal X-ray structure studies of $M_2XMo_{12}O_{42}^{n-}$ of Torchenkova et al. [76–78] have shown that the M sit on the C_3 axis of the anion on opposite sides of the ligand HPA attached to three terminal oxygen atoms from three adjacent MoO_6 groups.

Unfortunately, in most cases, the solubility problems prevent the measurement of the ^{17}O- and ^{95}Mo-NMR spectra in any detail [79,80], but the results do show that most Ln^{n+} and M^{n+} form very labile complexes (on the NMR time scale). The ^{95}Mo-NMR spectra show a gradual shift in the position of the single line as the ratio (Ln:lig) is changed [79]. If the two Ln cations were fixed on the surface of the polyoxoanion, we would expect two lines in the ^{95}Mo spectrum with the shifted one belonging to the Mo closest to the paramagnetic cation. The single line indicates a rapid migration over the eight possible coordination sites.

In contrast to the central atom which is bound to O_a oxygens which have sp^3 hybridization, the surface terminal oxygen atoms link only molybenum and the paramagnetic cation. This is a better route for spin transfer as we have observed for the $XW_{10}O_{36}^{n-}$ complexes.

Positive and negative ^{17}O-NMR shifts have been observed for Nd^{3+} and Ho^{3+}, respectively. In both cases, the lability of the complexes produce one averaged resonance [79].

This type of HPA can also serve as a ligand with d-elements [80,81]. As is the case for the lanthanides, many of the complexes are quite labile in solution and give rise to large isotropic shifts in the single resonance of the ^{95}Mo-NMR spectra of the Co^{2+}, Mn^{2+}, and Cu^{2+} complexes despite the presence of excess free polyoxoligand. The complex with Fe^{3+}, however, is found to be inert and the one broad line at 177 ppm has been assigned to those Mo atoms far from the Fe^{3+} ion. This shift is considered to be mainly dipolar in nature. The resonance line for the Mo atom close to the Fe^{3+} ion is too broad to be observed.

Labile complexes between lanthanide ions and the rather peculiar HPA Ni^{4+} $Mo_9O_{32}^{6-}$ (D_3 symmetry) have been studied. This anion has an octahedral configuration about the central metal atom with *cis*-MoO_2 terminal bonds with two types of MoO_6 octahedra. The terminal oxygen atoms form a triangular face in the coordination polyhedron about the Ln ion. Fedotov et al. [82] have found large deshielding shifts in the ^{95}Mo-NMR resonance for complexes with La^{3+} and Pr^{3+}. The gradual shift in the NMR lines with a change in the ratio (Ln:polyoxoanion) demonstrates the existence of a fast exchange between complexes and free polyoxoanions. No similar complexes with the d-elements has been observed but the broadening of the ^{17}O-NMR line assigned to the terminal oxygen atoms has been explained by ion-pairing [82] with the Ni^{2+} ion.

4.3. Electron density transfer in diamagnetic complexes

We have considered above only those cases where unpaired spin density is delocalized from paramagnetic cations onto ligand atoms. For example, Ni^{2+} (d^8) in octahedral coordination has its two unpaired electrons in e_g orbitals. Are these the only electrons transferred or is some of the electron density from the filled t_{2g} shell transferred as well? The ^{183}W-NMR of $PW_{11}Co^{3+}O_{39}$ with its six paired electrons in the t_{2g} orbitals could yield an answer to this question. In Section 7.3 we will consider this possibility for other HPA with diamagnetic central atoms.

Quite interesting cases of electron density delocalization onto neighboring ligand atoms have been observed for Ru^{2+} and $Mo(NO)^{3+}$ diamagnetic complexes with the lacunary $PW_{11}O_{39}^{7-}$ ligand [68,69]. The presence of the six electrons in the t_{2g} orbitals in $PW_{11}RuO_{39}(H_2O)^{4-}$ results in a positive shift for practically all of the ^{183}W resonances [68] (Fig. 6, Table 6). Naturally, the largest shifts are expected to be for the W atoms closest to the Ru^{2+} ion and the electron density is transferred by the π-mechanism.

Another example has been found for the diamagnetic $PW_{11}Mo(NO)O_{39}^{4-}$ complex [69]. Similar to the Ru^{2+} complex, the electron transfer should proceed through the W–O–W bridges and it may be assumed, as well, that the corner sharing ensures a more effective electron transfer. In both cases, the appearance of some electron density in the $W5d_{xy}$ orbital increases the paramagnetic contribution to the diamagnetic shift (see Eq. (1)), resulting in a positive chemical shift similar to that observed in two electron blues, which are considered in Section 6.1. The larger ^{183}W-NMR shifts for the Ru complex may be explained both by increased number of electron (d^6) (d^4 in the Mo complex) and by the electron withdrawal capability of the nitrosyl group. Thus the positive shift should be proportional to $1/\Delta E_{d^*-d^*}$.

The ^{17}O-NMR would be of great help for both of these cases to follow the pathway for the electron transfer and to evaluate the paramagnetic contribution to the diamagnetic shift due to the presence of electron density in the oxygen p-orbital (see Eq. (1)).

Recently small anions of the Lindquist structure type $M_5O_{18}(M^*NO)^{3-}$ have been studied by ^{17}O-, ^{95}Mo-, and ^{183}W-NMR [83]. In contrast to the Keggin derivatives the chemical shifts are smaller for these anions and correspond to

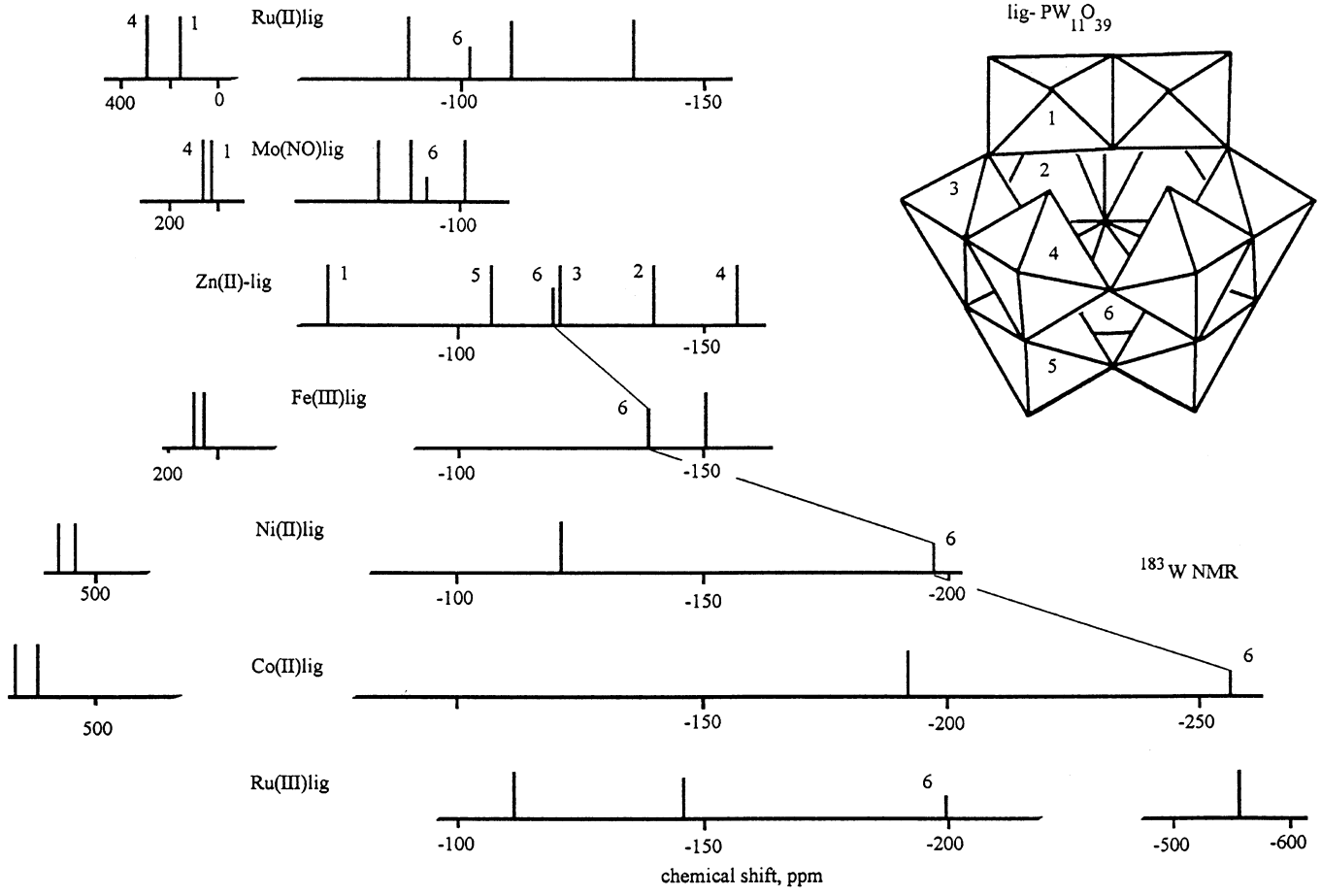

Fig. 6. The structure of $PW_{11}MO_{39}^{n-}$ and ^{183}W-NMR chemical shift diagram.

transfer between edge-sharing MO_6 octahedra (for ^{183}W it is $+109$ ppm relative to $W_6O_{19}^{n-}$ and $+93$ and $+196$ ppm for the edge and corner sharing transfer of the electron density in the Keggin derivatives, confirming the assignment of two lines to W_1 and W_4 atoms (Table 6, Fig. 6)). The ^{17}O-NMR lines belonging to the bridge M–O–M* is also positively shifted ($+33$ ppm) which might show a contribution from the $O2p_\pi$ orbitals to the electron density transfer onto the adjacent metallic atoms, but this value should be compared with a similar complex (charge and size of the introduced cation) with no electron density transfer involved. Surprisingly, some electron density is transferred to the apical tungsten atom ($+58$ ppm). Electron transfer through the internal common oxygen atoms is unlikely, but electron density should pass through the bridge M_c–O–M_t despite its rather bent character. Similar electron density transfer is observed for $LnW_{10}O_{36}^{n-}$, but the actual shift due to electron delocalization should account for the complexation (charge) contribution, also, because only a $+17$ ppm shift of ^{183}W line is observed for the apical tungsten in $VW_5O_{19}^{3-}$ [84].

5. Delocalization of electron (polaron) in polyoxometalate sphere

HPA whose structures are built from MO_6 octahedra of local C_{4v} symmetry may be reduced by one or more electrons giving rise to the intensely colored species—'heteropoly blues' [1,5]. Retention of the original structure upon reduction is due to the added electron occupying a non-degenerate d_{xy} orbital (Scheme I) which leaves all the bonding orbitals unchanged. The bridging oxygens present pathways for electron delocalization. Such heteropoly blues belong to a class of mixed valence complexes where optical and thermal intervalence charge transfers $M^{(m-1)+} \rightarrow M^{m+}$ may occur.

Spin delocalization in the reduced forms is believed to be governed by two parameters that act in opposite directions; the electron phonon coupling constant λ that favors localization and the electron interaction parameter ε that favors delocalization [23,26,27,85]. Both parameters depend upon the local geometry with λ being more or less the same for closely related molecules. The transfer integral, J, that accounts for the electronic interaction between adjacent cations depends largely on the M–O–M bond angle. J may be evaluated from the equation [26]:

$$E_{th} = 0.25E_{op} - J = (J/E_{op}) \quad (7)$$

where E_{th} is the energy of thermally activated electron transfer which is estimated from the temperature dependence of the EPR parameters and E_{op} is the optically activated intervalence charge transfer energy, found from the position of the lowest optical intervalence transition.

Although there are difficulties in determining the intervalence band position, rough estimates show that the electron hopping process is easier (E_{th} is smaller and J is larger) between corner shared octahedra. For example E_{th} is 0.155 eV and J is 0.15 eV for $Mo_6O_{19}^{3-}$ with edge-shared octahedra ($\angle$ Mo–O–Mo $\approx 120°$) while E_{th} is 0.035 eV and J is 0.34 eV for $PMo_{12}O_{40}^{4-}$ with both edge- and corner-shared octahedra ($\angle$ Mo–O–Mo $\approx 155°$) (Table 8 [25]).

Table 8
Calculated α, k, E_{th}, E_{opt} and J for heteropolyanions

Anion	α	k	E_{th} (eV)	E_{opt} (eV)	J (eV)	Ref.
$Mo_6O_{19}^{3-}$	0.90	0.74	0.155	1.13	0.15	[20]
α-$PMo_{12}O_{40}^{4-}$	0.77	0.58	0.035	1.07	0.34	
α-$GeMo_{12}O_{40}^{5-}$	0.79	0.69	0.045	0.913	0.25	
β-$SiMo_3W_9O_{40}^{5-}$	0.79	0.62	0.055	1.00	0.26	
α-$SiW_{12}O_{40}^{5-}$			0.035	1.00	0.31	[21]
α-$H_2W_{12}O_{40}^{7-}$	0.035	1.04	0.33			
$As_2W_{18}O_{62}^{7-}$			0.040	1.38	0.45	

The intensity of the intervalence charge transfer band is also higher in the last case. A more extensive interaction between two tungstens through the corner sharing oxygen atoms is also confirmed by a larger $^2J_{W-W}$ nuclear–nuclear coupling.

5.1. Unpaired spin in $XM_{12}O_{40}^{n-}$ ions with the Keggin structure

As we have seen, the highly symmetrical HPA of the Keggin structure, $XO_4M_{12}O_{36}^{n-}$, is built by four triplets of edge-shared oxygen (O_c) octahedra attached to each other by 12 vertex oxygens (O_b) forming a tetrahedron of oxygens (O_a) around the heteroatom [1,5] (Fig. 8). Twelve terminal and bridging oxygens usually give four lines in the ^{17}O-NMR spectra [10,86,87] which are fully consistent with the crystal structure. The lines of the terminal and bridging oxygen atoms are well separated but the lines of O_b and O_c are, sometimes, not well resolved due to the interaction of O_c with protons or solvent molecules. The small difference in the angle of the M–O–M bridge between corner and edge sharing units for units having nearly identical M–O distances of 1.91 Å results in this minor splitting of the b and c lines.

As mentioned above, the presence of a non-degenerate d_{xy} orbital for each octahedron allows these HPA to be reversibly reduced with one or more electrons with retention of the original structure [5]. The reduction of the anion results in the blue color due to the intervalence band $M^{(m-1)+} \rightarrow M^{m+}$ that appears in the near IR region (> 5000 cm^{-1}) [5].

The one electron reduced species give EPR spectra which have been interpreted as showing a complete delocalization of the unpaired spin over the 12 metallic atoms, which forms a polymetalate sphere [25,26,88] with a hopping frequency rate $> 10^8$ Hz [89]. The EPR spectra at different temperatures has shown that one electron is trapped at quite low temperatures with only a partial delocalization but is completely delocalized at higher temperatures. This suggests that the spin is partially localized in the ground state but is involved in a rapid thermal hopping from one site to another at elevated temperatures.

The HPA with one electron trapped at a single metallic site, e.g. in $XM_{11}^{6+}M^{5+}O_{40}^{n-}$, can be compared with the mixed HPA of the type $XM_{11}^{6+}Re^{5+}O_{40}^{n-}$, XW_{11}^{6+}

$Mo^{5+}O_{40}^{n-}$, or $XW_{11}VO_{40}^{n-}$ where the electron resides on a more easily reduced metallic cation [90–92]. The degree of electron delocalization in the ground state is determined by the extent of interaction in the bridges. Using EPR and optical parameters of the reduced anions, the mixing coefficient α for the Mo d_{xy} may be found. It has been shown that α decreases with increasing numbers of Mo–O–Mo bonds formed by corner-shared octahedra [25].

The situation of HPA containing two or three vanadium centers will be considered in more detail because it reveals some peculiarities in the bond patterns [27,29]. There are two possible modes for junction between adjacent VO_6 units, edge-shared and corner-shared. In the Dawson structures $P_2W_{16}V_2O_{62}^{9-}$ and $P_2W_{15}V_3O_{62}^{10-}$ two or three vanadiums occupy the sites in the polar triplet and have only edge-shared oxygens for electron delocalization, while in the anions $SiW_{10}V_2O_{40}^{7-}$ and $SiW_9V_3O_{40}^{8-}$ the vanadium atoms occupy adjacent sites in three different triplets so electron transfer may occur through corner-shared oxygen atoms. In the EPR of the two and three vanadium species, with one unpaired electron, the hyperfine splittings at r.t. show an equal distribution of the spin on all vanadium atoms for $P_2W_{16}V_2O_{62}^{9-}$ (15 lines from the two ^{51}V with nuclear spin of 7/2) and $P_2W_{15}V_3O_{62}^{10-}$ (22 lines) [24,29]. Lowering of the temperature (ca. 100 K) results in trapping of the electron on one vanadium but it is nevertheless partially delocalized ($J = 0.135$ eV) on neighboring vanadiums [29].

Protonation of the trisubstituted anion gives a 36-line hyperfine pattern in the EPR spectrum, showing that the electron interacts extensively with only two of the vanadium cations [24,29]. Analysis of the spectra have shown that the electron transfer between the two vanadiums connected to the protonated bridging oxygen atoms is absent. The frozen solution spectra of $P_2W_{15}V_3O_{62}^{10-}$ could be simulated by assuming that the unpaired spin is localized on one vanadium but has a superhyperfine interaction with the two equivalent vanadium atoms linked by the protonated bridge [29].

In the case of $SiW_{10}V_2O_{40}^{7-}$ an equal interaction of the electron with the two vanadium atoms is observed in the EPR spectrum of the solution, showing a 15-line hyperfine splitting [24,27]. The temperature dependence of the polycrystalline EPR spectra shows that the equality of the interaction between the two vanadium atoms, linked to each other by corner-sharing, is due to a hopping process [27]. Analysis of the results yield a rate constant for the hopping process of $7.0 \times 10^9\ s^{-1}$ at 300 K and $2.0 \times 10^9\ s^{-1}$ at 150 K. The 300 K rate is close to that found from relaxation data [70] for a single electron delocalized over three molybdenum atoms in $P_2W_{15}Mo_3O_{62}^{7-}$.

A more complex behavior has been observed in trisubstituted $Si(P)W_9V_3O_{40}^{8-(7-)}$ anions, whose solution EPR spectra consists of 43 lines [24,28]. The spectrum has been explained in terms of the electron interacting unevenly with the three vanadium nuclei. The temperature dependence (350–77 K) reveals no change in the hyperfine pattern in contrast to that found for $P_2W_{15}V_3O_{62}^{10-}$ where the electron is trapped at $T = 100$ K. This difference is thought to arise from the fact that the corner-shared V–O–V have a better d_π–p_π–d_π overlap than the edge-shared V–O–V and the non equivalence of the three vanadium atoms is believed to be due

to protonation at one of the bridging atoms even at very high pH. However, this non equivalence could be intrinsic in that corner-sharing makes the shoulders of the less bent V–O–V bridge substantially different, particularly when the M–O distance becomes large. In polyoxo tungstates the nuclear–nuclear coupling in such bridges can be markedly smaller than those observed for edge-sharing [93,94] and thus electron transfer may be partially hindered. For this reason, it is rather difficult to compare and interpret the results. Cadot et al. [93] have reinvestigated this case with $SiW_9V_3O_{40}^{8-}$ and have shown that uneven delocalization occurs even in completely deprotonated anion.

In general it may be assumed that the increase in the number of equivalent MO_6 octahedra facilitates electron delocalization. For example, the α-coefficient of the d_{xy} orbital decreases from 0.90 in $SiW_{11}Mo^{5+}O_{40}^{5-}$ to 0.79 in β-$SiW_9Mo_3O_{40}^{5-}$ to 0.77 in $SiMo_{12}O_{40}^{5-}$ due to an increasing degree of delocalization onto neighboring atoms [25].

The delocalized electron can be considered as a small polaron [25] whose thermally activated hopping frequency, estimated from EPR, is $>10^8$ Hz, However, such an electron only slightly polarizes the surrounding bonds as inferred from the analysis of the IR-spectra of the one electron reduced form [95].

In summary, the EPR spectra of the Keggin anion one electron blues have an isotropic spectra which shows a complete delocalization over the 12 metallic sites [25,26,88,89]. Lowering the temperature results in an anisotropic pattern corresponding to a trapped electron on one cation of the coordination sphere. Using the EPR parameters and optical data the coefficients of α for the d_{xy} orbital and k, the isotropic Fermi contact term, may be calculated and the degree of delocalization inferred (Table 8), the highest degree of delocalization is observed for $PM_{12}O_{40}^{4-}$, where k is smallest. As noted by So and Pope [24], the degree of delocalization increases in the series of metals $W < Mo < V$, along with the optical electronegativity.

The two electron reduced forms of the anions are diamagnetic. Complete delocalization for the electron pair may be regarded as a large bipolaron and this was first proven experimentally by the ^{17}O-NMR spectra of the reduced form of $SiMo_{12}O_{40}^{6-}$ [96]. Two electron reduced HPA will be considered in the next section.

The delocalization process in the one electron reduced forms produces short T_1 times making NMR detection of ^{17}O possible. Piepgrass et al. [87] have successfully measured the NMR in the paramagnetic one electron heteropoly blue, such as $XM_{12}O_{40}^{n-}$ (1e) and found them to exhibit quite interesting chemical shifts (Table 9) with non-equal interaction of the delocalized unpaired electron with different oxygen atoms similar to what has been observed in $Co^{3+}W_{12}O_{40}^{5-}$.

In calculating the paramagnetic shifts in these systems we take the diamagnetic Keggin anion as our diamagnetic reference and subtract it from the shift measured in the one electron reduced species. There is evidence in the NMR of the two electron blues [96–98] of a measurable change in the diamagnetic component of the shift due to the delocalized electrons. This can be corrected for by halving the difference in the NMR shift between the corresponding two-electron blue anion and the starting Keggin anion and subtracting this correction from the first estimate of

the paramagnetic shift. This analysis for the $XW_{12}O_{40}$ gives a positive shift for the bridging oxygen O_b of 55, 44, 45 ppm for X = Si, P, H_2, a negative shift of -135, -132, -160 ppm for the bridging atom O_c, and a negative shift of -118, -104, -98 ppm for the terminal O_d. The results for $PMo_{12}O_{40}$ are different for O_b and O_c with shifts of 161 and 14 ppm, respectively, and similar for O_d with a shift of -123 ppm. It should be noted that some shifts are solvent dependent.

The explanation for these shifts is difficult due to several modes of proposed spin delocalization. We can obtain an estimate of the dipolar contribution even though no data on $\chi_{\parallel}$ and $\chi_{\perp}$ is available for the one electron blues. We can use the ^{31}P-NMR data [70] for $P_2W_{17}Mo^{5+}O_{62}^{7-}$ where Mo^{5+} is in the same environment. The estimated δ_{dip} values do not exceed -10 ppm for O_d and $+3$ ppm for the O_c and O_b bridging oxygens, if the chemical shift for P_b located in the unperturbed half of the Dawson anion is assumed to be entirely dipolar. A negligibly small dipolar contribution is also confirmed by the insignificant shift of the oxygen line assigned to the internal tetrahedron XO_4.

One mechanism is the direct interaction between the occupied d orbital of the metal atom center with the oxygen orbitals. Only the p_π orbital of the bridging oxygen atoms lying in the *xy*-plane can interact directly with the $W^{5+}5d_{xy}$ orbital and the degree of this interaction is strongly dependent on orbital overlap, which in turn depends on the distances and angle in M–O–M. To get an isotropic contact shift requires some admixture of the s orbital with p_π. According to the homonuclear coupling, $^2J_{W-W}$, observed in the ^{183}W-NMR of non-reduced polyoxo-

Table 9
The ^{17}O-, ^{31}P-, and ^{183}W-NMR chemical shifts[a] for Keggin anions

Anion	O_a	O_b	O_c	O_d	P	W	Ref.
$PMo_{12}O_{40}^{3-}$[b]	80	551	583	937	−0.4		[87]
$PMo_{12}O_{40}^{4-}$ (1e)	80	706	567	784	3.5		
$PMo_{12}O_{40}^{5-}$ (2e)	70	539	523	878	−3.3		
$PMo_{12}O_{40}^{3-}$		530	590	945	−4.0		[97]
$PMo_{12}O_{40}^{4-}$ (2eH)		525	429	941	−6.0		
$PMo_{12}O_{40}^{5-}$ (2e)		525	514	900	−4.6		
$SiMo_{12}O_{40}^{4-}$		551	572	936			[96]
$SiMo_{12}O_{40}^{6-}$ (2e)		520	520	897			
$PW_{12}O_{40}^{3-}$		406	428	766	−14.6		[87]
$PW_{12}O_{40}^{4-}$ (1e)		447	266	632	−10.4		
$PW_{12}O_{40}^{5-}$ (2e)		401	369	705	−17.6		
$SiW_{12}O_{40}^{4-}$	25	404	417	763		−103[c]	
$SiW_{12}O_{40}^{5-}$ (1e)	31	451	261	627			
$SiW_{12}O_{40}^{6-}$ (2e)	29	388	375	727		−43[c]	
$H_2W_{12}O_{40}^{6-}$	81	408	498	723		−113[c]	
$H_2W_{12}O_{40}^{7-}$ (1e)		451	273	581			
$H_2W_{12}O_{40}^{8-}$ (2e)		405	368	676			

[a] Measured relative to $H_2^{17}O$ and $Na_2^{183}WO_4$, respectively, in aqueous solution at 330 K.
[b] Measured in CD_3CN.
[c] The ^{183}W shift [95].

tungstates [12], the interaction in $W–O_b–W$ is twice as strong as that in $W–O_c–W$ (20 viz. 10 Hz, respectively) despite the smaller W···W distance in the latter case. This may explain the existence of the positive shift observed for O_b.

Theoretical considerations [15,32] have predicted the possibility of spin polarization of the spin density of paired electrons in filled MOs which would produce the negative shift observed for two of the oxygens. It could be postulated that the difference in the shifts for the bridging oxygens in $PMo_{12}O_{40}^{4-}$ (1e) relative to that in the tungsten analog is due to either a larger direct spin density transfer for the Mo anion or to a larger spin polarization in the case of the W anion due a greater use of the W 6s orbital.

It should be noted that there is a rather small paramagnetic shift for both the ^{31}P-NMR [97] and the ^{17}O-NMR of the O_a oxygen, which are far from the metal sites on which the unpaired electron resides.

Fluorotungstates of the general formula $H_{1,2}W_{12}F_xO_{40-x}^{n-}$ with the Keggin structure having $x \leq 3$ have been made [99] in which the fluoride ion replaces the O_a oxygen of the internal tetrahedron. EPR data for the one electron reduced species at r.t. give no indication of the method for delocalization of the unpaired spin. From the analysis of the EPR spectra at low temperatures, it has been deduced that the electron is trapped on the tungsten atom of the triplet that has no F^-. Increasing temperature broadens the signal and the question as to whether the spin remains localized or becomes delocalized remains open. The ^{17}O-NMR may clarify this interesting point.

5.2. Unpaired spin in $X_2M_{18}O_{62}^{n-}$ with the Dawson structure

When the HPA contains two or more structurally different types of MO_6 octahedra, both of which have a local symmetry close to C_{4v}, there is the possibility of preferential (de)localization of any additional electrons introduced into the system. As can be seen in Fig. 7, there are two types of M atoms in the Dawson anion and the ^{183}W-NMR for the polyoxotungstates clearly shows this difference by the large chemical shifts (-127 ppm for the three MO_6 labeled 1,8,9 (or A in Fig. 10) versus -173 ppm for the six MO_6 in the belt region (labeled 2–7 in Fig. 7 or B in Fig. 10) [11]). Analysis of the EPR spectra of the one electron reduced $X_2M_{18}O_{62}^{n-}$, at low temperatures, shows the electron to be trapped at one tungsten atom in the six-membered belt [26,89]. Increasing temperature, however, results in an increased mobility in the unpaired electron but the exact distribution cannot be deduced from the EPR data only. Three possibilities are suggested by the EPR data: (1) the electron is on two adjacent WO_6 linked to each other by a mirror plane perpendicular to the C_3 axis, (2) the electron is delocalized over the two belts, and (3) the electron is delocalized over the whole structure but with different lifetimes on the different types of WO_6.

The positive shift in the ^{31}P-NMR for the reduced anion $P_2W_{18}O_{62}^{7-}$ (in solution) is almost equal to the average of the two ^{31}P shifts in α_1-$P_2W_{17}Mo^{V}O_{62}^{7-}$, where the Mo occupies one of the belt octahedra [70]. This may be an indication that the electron is delocalized in the two belts of $P_2W_{18}O_{62}^{7-}$. Further the line width of the

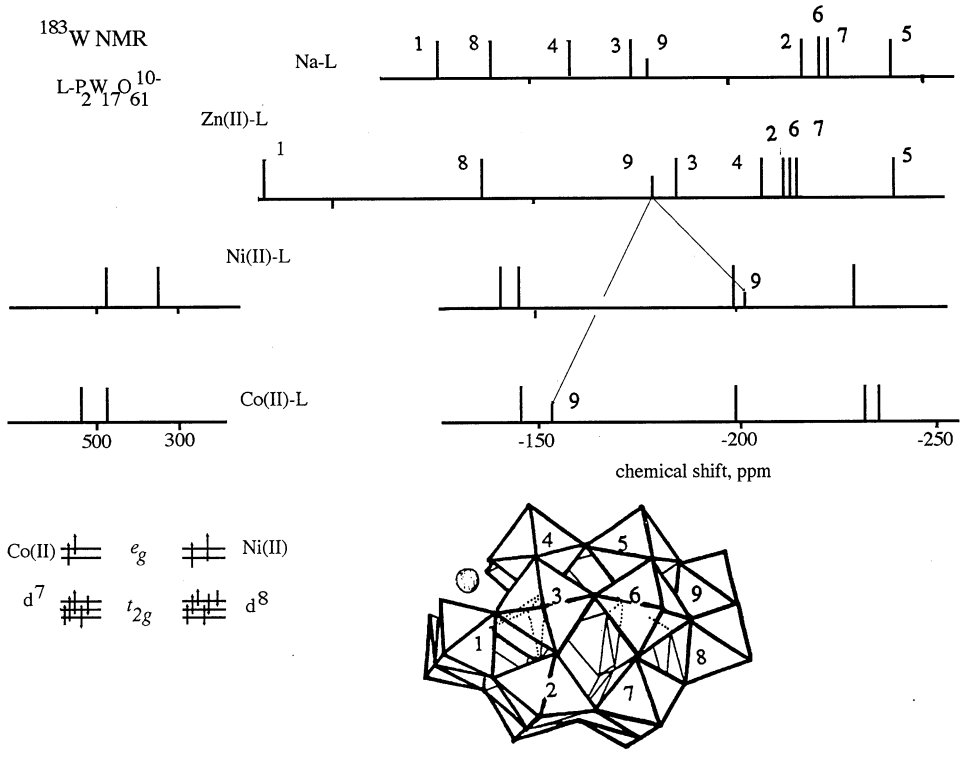

Fig. 7. The structure of α_2-$P_2W_{17}MO_{61}^{n-}$ and ^{183}W-NMR chemical shift diagram.

^{31}P-NMR line has been used by Kozik et al. [70] to estimate the hopping frequency of the electron to be 1.7×10^{11} Hz. Using UV-spectra we may speculate that the position of the W $5d_{xy}$ orbital in the A octahedra to be 4000 cm^{-1} higher than in the B octahedra, making thermal activation of the electron from the B octahedra to the A octahedra highly unlikely. Additional confirmation for delocalization over the belt octahedra has been obtained [100] from ENDOR studies of $NaH_2W_{18}F_6O_{56}^{7-}$, a close structural analog of $P_2W_{18}O_{62}^{7-}$, where the fluorine atoms are in the belt octahedra and the electron is found to be trapped in one of these despite the presence of the F^-. In this system $g_{\|} > g_{\perp}$, which is unusual for this type of polyoxoanion [27,89]. This is characteristic of three corner shared oxygens which gives rise to a very effective pathway for electron delocalization lowering the LCW transition, which in turn increases $g_{\|}$ value [8]. The same situation has been found for a new HPA $Cl_2W_{18}O_{62}^{5-}$ with one unpaired electron [101].

In contrast to the behavior of $P_2W_{18}O_{62}^{6-}$ the intrinsic chirality of $P_2Mo_{18}O_{62}^{6-}$, due to the deformability of the Mo–O–Mo bonds, results in the transformation of the one electron HPA into the oxidized parent and a two electron blue [102]. Barrows and Pope [103] have reexamined the electrochemistry of $P_2Mo_{18}O_{62}^{6-}$ in acetonitrile and have obtained the one electron reduced form. Once again the

electron is found to be trapped at low temperatures on a molybdenum in the belt octahedra ($g_{\|} > g_{\perp}$) and at higher temperatures electron hopping is observed (10^{10} Hz) between the mirror related belts of the Dawson structure. Though the ^{95}Mo-NMR of $P_2Mo_{18}O_{62}^{6-}$ does not show the expected two line spectrum for the two types of molybdenum (only the more intense line is seen [93]), we can assume that the difference is enough to restrict the delocalization to the equatorial belt.

Quite unexpected results have been obtained for the polyoxo molybdate $S_2Mo_{18}O_{62}^{5-}$ with the Dawson structure reduced by one electron [105]. The Mo^{5+} EPR spectrum at 253 K reveals 91 equally-spaced lines consistent with the assumption of a uniform distribution of the unpaired electron density. It has been argued that the electron delocalization is due to the absence of chirality in this anion giving rise to and equalization of the two types of molybdenum atoms. Surprisingly, an extremely low activation energy of 0.0045 eV was estimated for this system, because quite low values have been usually observed for tungstates.

Recently, Kortz and Pope [106] have solved the structure of the 18-molybdopyrophosphate anion $P_2O_7Mo_{18}O_{54}^{4-}$ (D_{3h} symmetry) which resembles the structure of $H_2As^{III}W_{18}O_{60}^{7-}$ (D_{3d} symmetry) if two different heterocenters are ignored [27]. They may be represented as two fragments of the Keggin anion without a triplet fused by corner sharing in eclipsed and staggered positions, respectively. All MO_6 octahedra have two edge and two corner shared oxygens, as in the Keggin anion and therefore the EPR spectra [106] for a frozen state is quite normal with $g_{\|} < g_{\perp}$ [27,89].

The most notable feature of this polyoxomolybdate anion is the extremely long $Mo–O_a$ bonds for a cap triad. It is probably due to the decreased P–O–P distance. At high temperatures the isotropic EPR spectrum indicates a thermal hopping process. Authors [106] assumed localization of the 'frozen' electron at one of the molybdenums in the polar triad which delocalizes over the triad at higher temperatures or is nearly evenly trapped in both polar and belt sites. Unfortunately, the ^{95}Mo- and ^{17}O-NMR of this anion are not available, at present, and this assumption must be regarded as tentative. The ^{31}P-NMR has been obtained but is not very informative.

6. Delocalization of electron pair (bipolaron)

The reduction of HPA is not limited to one electron. Up to 36 electrons may be introduced into the Keggin anion [5]. In most cases the reduction due to increasing electrons is accompanied by protonation of HPA, especially the molybdates, which facilitates the introduction of subsequent electrons. The two electron reduced forms of $XM_{12}O_{40}^{n-}$ (2e) are completely diamagnetic [107] and despite the probably strong Coulombic repulsion the second electron is thought to reside on an M atom adjacent to the M atom on which the first electron was trapped.

The situation of the electron pair is very similar to the bipolaron delocalization in the mixed valence oxides, especially WO_{3-x}, studied by Salje [108]. At present we are not able to say for the case of complete localization of two electrons in $P_2W_{16}Mo_2^{5+}O_{62}^{8-}$, whether the electrons are paired or not. Two electrons in

trisubstituted anions are known to be completely paired [107]. However, in the case of the two electron reduced Keggin anion α-$SiW_{16}V_2^{4+}O_{40}^{8-}$ with two adjacent vanadiums, the electrons are unpaired and exhibit no substantial magnetic interaction [27]. For the isomeric anion γ-$SiW_{10}V_2^{4+}O_{40}^{8-}$ (2e) in EPR spectrum only a broad resonance line is observed [109]. In this anion two adjacent vanadiums are joined by two bridging oxygen atoms where the two V d_{xy} orbitals are coplanar, which has been thought to give a good interaction [110].

However in the γ-$SiW_{10}W_2^{5+}S_2O_{38}^{6-}$ where $O{=}W^{V}W^{V}{=}O$ entity also acts as 'electron sink' two electrons are completely paired giving rise to a diamagnetism [110]. But two electrons in $SiW_9V_3O_{40}H^{7-}$ are coupled but not completely [24] in contrast to $P_2W_{15}Mo_3O_{62}^{8-}$ (2e) where two electrons are paired and evenly delocalized over the triplet Mo_3 [70]. We assume that the electron pair becomes mobile when the number of introduced cations is ≥ 3 and are paired. This delocalized electron pair will be named a bipolaron.

Unfortunately, there are no examples of two reduced addenda atoms separated by either the Mo^{5+}–O–W–O–Mo^{5+} or the Mo^{5+}–O–W–O–W–O–Mo^{5+} chains. Also no cases of both polar W_3 triplets being replaced by Mo_3 triplets $P_2W_{12}Mo_6O_{62}^{8-}$ each containing a mobile electron. Therefore we cannot confirm or discard the assumption of long range super-exchange with complete pairing of two electrons at such large distances.

A very large polyoxo anion $P_2W_{15}O_{49}$–$Zn_4O_{14}(H_2O)_2$–$O_{49}W_{15}P_2$ which consists of two large ligands separated by the $Zn_4O_{14}(H_2O)_2$ layer is an interesting case [65,111]. This anion after reduction by two electrons might have one electron in each half when the distance between two possible sites might be quite large to avoid the Coulombic repulsion, but from the interpretation of the ^{31}P-NMR spectra it was deduced that the electron pair migrates from one side to the other via a concerted penetration of the Zn layer with the intramolecular rate of 2×10^3 s^{-1} at 300 K [111]. The four electron reduced form has two pairs of electrons separated by the oxide layer.

From our point of view, the long range interaction should not be sufficient to force the spins to be completely paired. The energy of unpairing two electrons can be estimated as 1000–2000 cm^{-1} from the blue shift of the first intervalence $M^{(m-1)+} \rightarrow M^{m+}$ band for the two electron blue anion when compared to the one electron form. The delocalization of the electrons over the structure reduces the Coulombic repulsion but the pairing energy still keeps the electrons paired. The latest theoretical approach to the behavior of the electron pair in a trinuclear system is given by Borsch and Girard [112] and involves several mechanisms for delocalization.

6.1. Electron pairs in the Keggin anions

Introduction of the second electron into the anions $XM_{12}O_{40}^{n-}$ with the Keggin structure results in a diamagnetic system with two delocalized electrons. In some cases the two electron reduced forms give sometimes a weak EPR signal in a frozen solution (intensity $< 1\%$) which could be due to a probable minor impurity. For an

excited triplet state the transition should be observed in the half field region in EPR spectrum. Complete delocalization of the electron pair was first shown by the observation of a large high field shift in the three ^{17}O-NMR lines of silicomolybdate (2e) [96] relative to the oxidized parent. This pattern may be evidence of a complete and uniform distribution of the electron density (electron pair or bipolaron) over all MO_6 octahedra within the NMR time frame. The same behavior was later found in other polyoxo molybdates and tungstates with the Keggin structure [69,87,98] (Table 9). ESCA and other data [5,13] have shown, in this case, that we are dealing with two electrons in d^1 orbitals and not with a d^2 configuration.

In considering these NMR chemical shifts, the importance of the contributions of different excited states to the paramagnetic term in Eq. (1) should be examined. The reduced state of the MO_6 octahedron under consideration has one electron in the M d_{xy} orbital (see Scheme I). The main contribution for ^{17}O and ^{183}W shifts in the oxidized parents comes from the states resulting from the promotion of an electron from the bonding and nonbonding MOs into the antibonding MOs, which are localized on the metal cations. For the reduced forms, these states and the ones coming from $d^* \rightarrow d^*$ transitions contribute mainly to the metal NMR shifts and contribute little to the oxygen shifts. For the reduced form, the additional electrons produce an extra charge distribution in the metal d_{xy} orbitals that would displace the position of the CT bands to higher energies (of about 1 eV) due to the repulsion of the electron excited from an occupied MO. The increased ΔE decreases the contribution from the paramagnetic term in Eq. (1). It can be estimated that the localization of one electron at the metallic site would shift the lines about 580 ppm for O_d and 360 ppm for O_b and O_c from the correlation between δ and $1/\Delta E$ [10]. The averaging of two electrons over 12:12:12 oxygen atoms, would give shifts around -20, -15, and -20 ppm, respectively. These are close to the observed shifts (Table 9) but the possible contribution of the $d^* \rightarrow d^*$ transitions were not taken into account.

Certainly, we should account for the change of the overall charge of the reduced species. For example, the lines for the terminal and bridging oxygen atoms are negatively shifted going from $PW_{12}O_{40}^{3-}$ (766 and 420 ppm) to $PW_{10}V_2O_{40}^{5-}$ (726 and 403 ppm), respectively [113]. So this type of contribution should be taken into consideration in determining the shifts induced by the change in the paramagnetic term.

The equivalence of all W atoms in the reduced $SiW_{12}O_{40}^{6-}$ (2e) with a delocalized electron pair (bipolaron) was confirmed by the observation of a single ^{183}W-NMR line which is deshielded relative to the oxidized parent by 60 ppm [107] (Table 9). It would seem that the shielding of the reduced W should increase with the increase of electrons and this would be true, also, for the ^{17}O-NMR resonance. Kozik et al. [107] have tried to account for the deshielding of the reduced W^{5+} by estimating both the diamagnetic and paramagnetic components in the theory of the shift. The paramagnetic shift was estimated from the extrapolation of the correlation [11] of δ to λ (the wave length in nm) for the mean ΔE of two $d^* \rightarrow d^*$ transitions ($\sim 13\,000$ cm^{-1}) and the diamagnetic part was estimated from the negative shift of W in the triplets which do not receive electrons in the reduced Dawson anion

$P_2W_{18}O_{62}^{8-}$. A more detailed consideration to the problem will be given in Section 6.2.

NMR experiments can only give a lower limit to the hopping rate of the delocalized electron pair. The large difference, however, in the IR spectra between the one and two electron reduced forms [95] suggests the rate is comparable to the molecular vibrations and may be as large as 10^{13} Hz. It had been assumed that if the distance between the electrons were large, the hopping process would have little effect on the IR absorption but actually a substantial background is observed and the bridging vibrations are smeared. Other experiments are needed to clarify this point.

A quite interesting feature of the problem of electron pair delocalization arises when the symmetry of the Keggin anions is reduced. For example, if one or two of the triplets is rotated 60° giving rise to β and γ isomers an uneven distribution of the electron pair may be deduced from the ^{17}O-NMR spectra [96,97] with the larger distribution over the six-member belt in the β-isomers.

In γ-$SiW_{12}O_{40}^{4-}$, two unique tungsten atoms linked to each other by the edge and with almost perfect coplanarity of the W5d_{xy} orbitals are found to be quite shielded (− 165 ppm) (Fig. 9a).

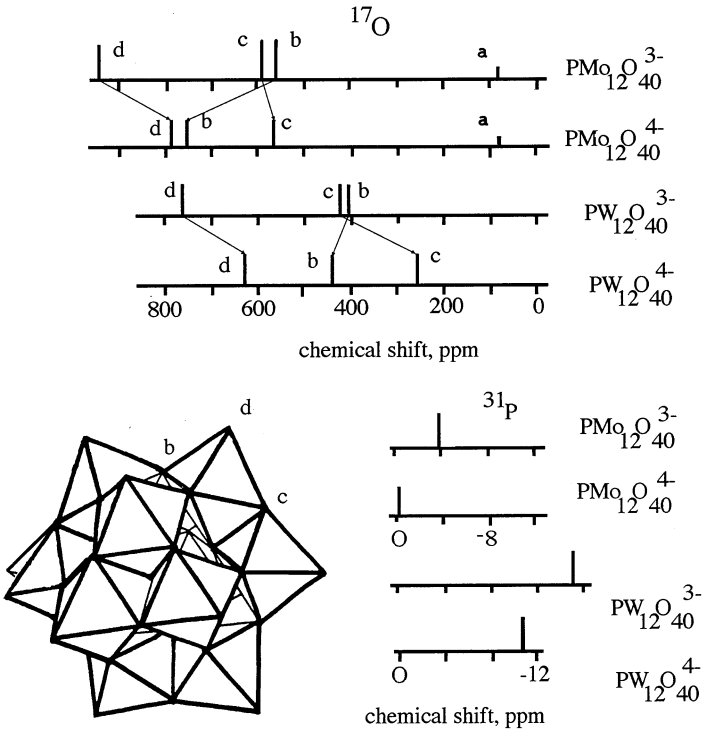

Fig. 8. The Keggin and ^{17}O- and ^{183}W-NMR chemical shift diagram

The other tungsten atoms give rise to three lines with an intensity ratio of 4:2:4 and shifts in the range of -100 to -127 ppm [114]. From the correlation between the ^{183}W shifts and the $\langle g \rangle$ values of the one electron blues [8], it has been deduced that these unique tungstens do not accept the reducing electrons. They may be localized on one of the two nearest tungstens or on the four furthest ones opposite to the unique tungstens. Delocalization over the four equivalent adjacent tungstens at the opposite side is confirmed by the large shift of the ^{183}W lines, ranging from -127 to $+489$ ppm. The other lines undergo small positive shifts indicating small partial delocalization onto these atoms.

We would like to consider the shifts induced by a change in the anionic charge. If it would be possible to find an anion with two, for example, vanadium atoms in the $4M_A$ array, we could see their influence on the position of the corresponding lines. But only γ-$SiW_{10}V_2O_{40}^{6-}$ with two vanadiums sharing an edge (D sites) has been prepared, and they induce high field shifts for all three ^{183}W-NMR lines despite the edge sharing that should give rise to deshielding of the nearby tungsten [114]. Thus the actual shifts induced in tungsten atoms, which do not accept electrons, by the introduction of the two electrons are not known. We may safely propose that the electron pair is locked in the $W_{2B}W_{2A}W_{2A}W_{2B}$ 'bath' without putting any electron density into the four separately located tungsten atoms (C and D sites).

Thus in a case of limited delocalization in γ-$SiW_{12}O_{40}^{6-}$ (2e) [114], the electron pair will induce a shift in the ^{183}W line from $\delta(W^{VI}) = -127$ to $+489$ ppm. Using the relation:

$$\{2\delta(W^{V}) + 2\delta(W^{VI})\}/4 = +489$$

we can estimate the $\delta(W^{V})$ value to be 1105 ppm.

We now consider the delocalization of the electron pair in the decatungstate $W_{10}O_{32}^{6-}$ which has two distinct types of tungsten atoms in two square arrays and has two apical atoms (Fig. 9b).

In the oxidized form this anion displays two lines with a 4:1 intensity ratio [115–117] and whose ^{183}W-NMR shifts depends upon the solvent [116–118]. According to EPR data the reduction of this anion by one electron has the electron delocalized between two sets of tungsten atoms which are bound by linear bridges W–O–W. As the temperature increases, the electron begins hopping to other tungstens. Using EPR on a single crystal, Yamase [119] has found a hyperfine interaction of the electron with eight protons showing, indirectly, that the unpaired electron is delocalized over eight adjacent tungsten atoms.

Addition of the second electron results in their complete pairing, but published ^{17}O- and ^{183}W-NMR spectra for the two electron species are markedly different in two papers [116,117]. Duncan and Hill [117] have found spectra which coincide with the shift pattern expected for the reduced anions (Fig. 9b) when two electrons are completely delocalized over 8 tungsten atoms in the square arrays as deduced from a substantial positive shift of lines with an intensity of 4. A small positive shift in the W_a line with an intensity of 1 should not be taken as evidence for delocalization of some electron density onto these tungsten atoms. Imagine the

introduction of two pentavalent atoms into the two square arrays, it would induce a positive shift for both types of tungsten atoms as indicated in Fig. 9b (broken lines) because this edge sharing can be compared with the case of $VW_5O_{19}^{3-}$ where two tungsten lines are shifted to low field by about $+14$ ppm [84]. We can expect the actual shift would be slightly less for the 8 W and there would be no shift for the apical tungsten in the reduced form. In such considerations, the apical tungsten do not receive any electron density from the reduced tungsten. In general we can assume the electron pair in the delocalized state resides on tungsten atoms in equivalent surroundings.

Usami and Yamase [117] have measured a two line pattern with chemical shifts in the range of -80 to -90 ppm in experimental conditions in which one must assume the coexistence of several protonated species of both the two electron reduced $W_{10}O_{32}^{6-}$ and the one electron reduced form. The amount of the latter is quite small but in the case of a fast exchange between the one and two electron species, it may substantially change the position of the lines. ^{183}W-NMR cannot be observed for the one electron blue where each tungsten experiences 1/8 of an electron, but in the case of a fast exchange and a very small concentration (we estimate it to be not more that 1/1000) of the paramagnetic form it is possible to observe the ^{183}W-NMR for the two electron diamagnetic species. The ^{17}O-NMR spectrum of the solution reveals that the two electron form is the dominating one but the protonation of the anion induces some shifts of the lines. A study of the one electron form with ^{17}O-NMR would be desirable to follow the electron delocalization, as it has been done for the one electron species of the Keggin structure [87], to estimate the exchange rate for the two electron species. Moreover an effect of the counter-cation and medium on the chemical shift should not be overlooked and checked.

So in delocalization of the electron pair over six tungsten atoms the observed chemical shift at 390 ppm corresponds to the averaged one and using the relation:

$$390 = [-25 \times 6 + 2\delta(W^{V})]/8$$

the chemical shift δ is estimated to be about 1500 ppm, depending on solvent.

But for other reduced anions, for example α-$SiW_{12}O_{40}^{6-}$ with 12 equivalent octahedra, the ^{183}W-NMR line shifts only from $\delta(W^{VI}) = -103$ to -43 ppm [107] when the bipolaron delocalizes over the 12 tungsten atoms. Using the relation:

$$\{2\delta(W^{V}) + 10\delta(W^{VI})\}/12 = -43$$

we can estimate the value $\delta(W^{V})$ to be $+257$ ppm, which is believed to be quite small. This problem will be considered in the next section.

6.2. Electron pair in $X_2W_{18}O_{62}^{n-}$ and the existence of the spin bipolaron

In the HPA of the Dawson structure, two Keggin fragments (Fig. 10) are combined by six corner shared oxygens and it has been shown that the additional electron in the reduced form is delocalized but becomes localized at quite low temperatures [21,79] on one of the belt tungstens.

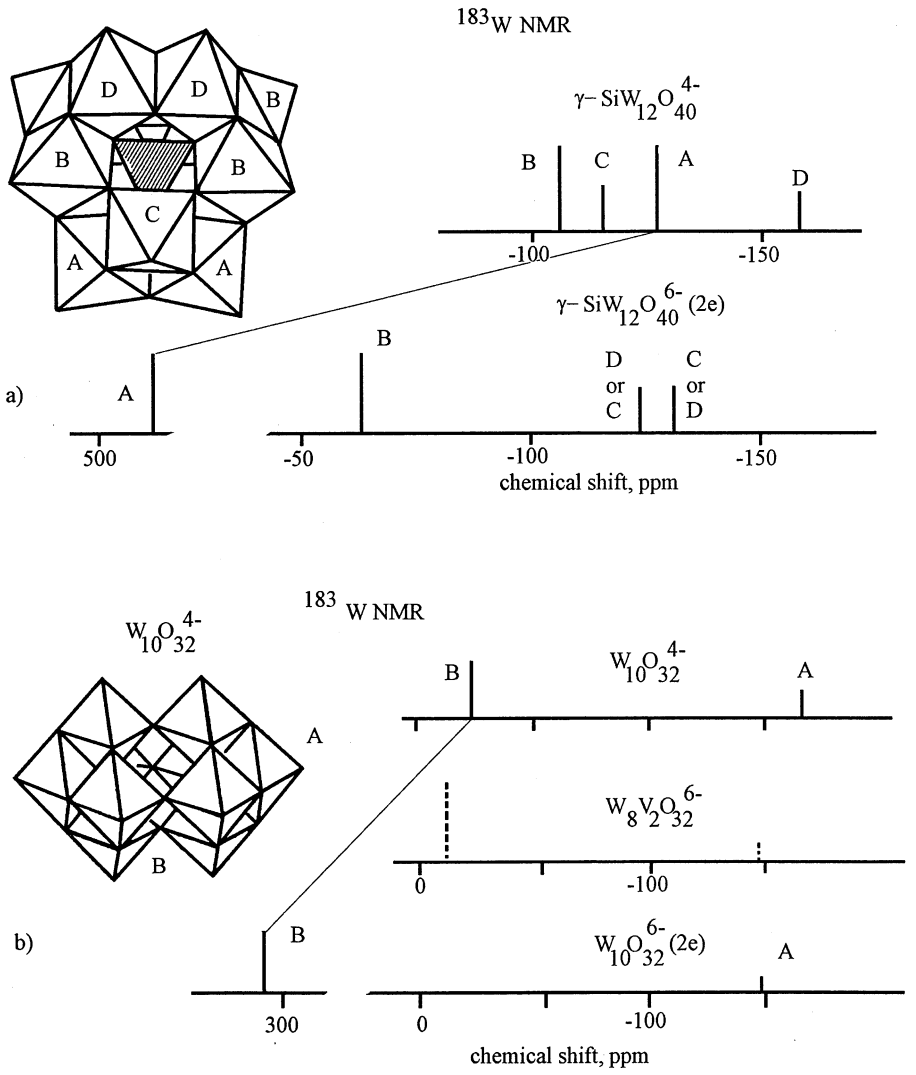

Fig. 9. (a) γ-$SiW_{12}O_{40}^{n-}$ anions and ^{183}W-NMR chemical shift diagram. (b) $W_{10}O_{32}^{n-}$ anions and ^{183}W-NMR chemical shift diagram.

The large down field shift of + 122 ppm [107] in the ^{183}W-NMR of the two belts consisting of 12 octahedra has been taken as evidence for the delocalization of the bipolaron on these atoms. The other six atoms which do not accept the additional electrons have a negative shift of − 172 ppm. This value was taken as normal shielding for the reduced systems but the substantial negative shifts (− 56 ppm) for the belt tungstens in the unreduced mixed $P_2W_{15}V_3O_{62}^{9-}$ HPA [120] has shed doubt on this assumption. It is well known that the tungsten nucleus has a high sensitivity to the site symmetry and to the charge on its neighbors [94].

The delocalization of the bipolaron strongly polarizes the oxygen atoms in the six-member ring and in a triplet and this in turn polarizes the paired electrons in MOs involving the triplet atoms. In this case we may regard this delocalized polarization as a *spin bipolaron* [121] as originally suggested by Mott [122] in explaining the superconductivity in oxide systems.

Indeed the position of the ^{183}W-NMR line for the two electron reduced HPA is determined by the change in the paramagnetic term in the chemical shift equation. The moving of the CT band to higher energies could decrease the σ_p of ^{183}W-NMR about -400 ppm as has been estimated from an extrapolation of the dependence of the δ/λ term It is possible that the $d^* \rightarrow d^*$ transitions for the d^1 electron could make a contribution but no estimation can be made because we have no information. Also the estimation from the plot of δ/λ requires a large extrapolation to quite low energies and could have large errors.

At the present time we cannot separate the chemical shift into contributions from the bipolaron and spin bipolaron due to the uncertainties involved. Moreover we need to remember that the value of the chemical shift induced by the spin bipolaron might be different for nuclei linked by corner and edge sharing.

In contrast to the polytungstates with the Dawson structure, which have the electron pair delocalized in two six-member belts, the two electrons in $P_2Mo_{18}O_{62}^{7-}$ show an identical distribution over both halves, as evidenced by a single ^{31}P-NMR line, but the ^{17}O-NMR has been interpreted to indicate that the electrons are immobile and are distributed over the four Mo atoms from the two belts that are linked to each other by corner sharing [123]. The electron localization has been indirectly deduced from the IR spectrum observed by Garvey and Pope [124], which does not show the characteristic features associated with delocalization [95]. These polymolybdates with the Dawson structure need further careful study as the delocalization process could be hindered by strong protonation on the anion by even one proton [106].

It should be mentioned that all these studies have tacitly assumed no type of isomerization of the anion structure has occurred upon reduction. In many cases this has been true for the tungstates [5].

6.3. Electron pair in mixed anions

Some insight into the chemical shifts caused by the electron pair introduced by reduction can be obtained by examining the shifts in the mixed anions. It has not been possible to replace any of the belt tungstens with M^{5+} cations with the configuration d^0, such as Nb^{5+}, but it has been possible to replace the polar triplet with Mo ($6+$ and $5+$), Nb^{5+}, and V^{5+}. The similarity of Mo to W results in two partially resolved lines at -179 and -180 ppm in the ^{183}W-NMR spectrum assigned to B(C) tungsten atoms in $P_2W_{15}Mo_3O_{62}^{6-}$ (Fig. 10). Addition of two electrons by reduction produces a splitting and a large negative shift of the B and C resonances [107]. In the following analysis, it will be assumed that the additional electrons are delocalized over the three molybdenums. Examination of only the NMR spectrum of the parent and reduced derivative would give the impression that

the B and C atoms experience similar negative shifts but this can be misleading, as we shall see when we examine the other mixed anions.

Finke et al. [125] have shown that in $P_2W_{15}Nb_3O_{62}^{9-}$, where the W_3 triplet is replaced by Nb_3, the B and C lines are separated with B shifted to -225 ppm even though the B atoms are separated by four bonds from the Nb atoms. Similar shifts were observed for $P_2W_{15}V_3O_{62}^{9-}$, which shows the importance of size and charge of a substitutant on the ^{183}W-NMR chemical shifts. If we were to assume the added two electrons in the reduced anion $P_2W_{15}Mo_3O_{62}^{8-}$ were localized on two of the three Mo atoms, we would predict that the spectrum would be that shown in Fig. 10(c) in which the shifts were taken to be two thirds of the shifts observed in $P_2W_{15}Nb_3O_{62}^{9-}$. The difference between this spectrum and the experimental spectrum can then be attributed to the delocalization of the electron pair over all three Mo atoms. It will be noticed that the closest atoms, B, are shifted the most and those furthest, A, the least. Thus the bipolaron induces chemical shifts of -132, -56, and -11 ppm in B, C, and A, respectively.

Unlike the unsymmetrical anions discussed above, the bipolaron in symmetrical anions like $XM_{12}O_{40}^{n-}$ (2e) is delocalized giving an average chemical shift for all of the tungsten nuclei. Looking along the C_3 axis, we can imagine three layers: triplet of three edge shared octahedra, linked to a hexa-ring by corner sharing. The latter is bound with a triad by edge sharing. Assuming that the electron pair is delocalized over the six-member ring, it will induce a spin bipolaron delocalization in the triplet and this may give rise to shift of at least -344 ppm. So without accounting for the contributions to other tungsten atoms, we can use the relation:

$$\{2\delta(W^V) + (-103 - 344)3 + (-103)7\}/12 = -43$$

and obtain a $\delta(W^V)$ value of $+773$ ppm, which seems quite reasonable.

It should be mentioned that the smaller the corner sharing the smaller the probability of forming a spin bipolaron. That is why the calculated shift for W^v in $W_{10}O_{32}^{6-}$ is quite large, because there is only one corner sharing occurring per octahedron.

It has been suggested [126] that the excessively large diamagnetic susceptibility in these polyanions is due to ring currents and this might appear to be a reasonable way to account for these delocalization shifts, which are of the proper sign. This would also explain the large shift in the A atoms in $P_2W_{18}O_{62}^{8-}$, where the large plus shift for the B atoms is evidence of shielding by the additional electrons delocalized over the two belts of six atoms which in turn generate large ring currents that produce the large negative shift observed for the A atoms. Unfortunately, calculations show this shift can not exceed several ppm in magnitude and cannot account for the observed large negative shifts.

A case of preferential delocalization may occur in the mixed $P_2W_{12}Mo_6O_{62}^{6-}$ anion, where one each of the Mo are in each triad and two Mo are in each belt. All are clustered together and are linked by corner sharing. Two of the Mo are connected to their nearest neighbor tungsten atom by edge sharing while the four belt Mo atoms are linked to their nearest neighbors by corner sharing. This structure accounts for the three tungsten NMR lines in the ratio of 4:4:4 [127].

After the two electron reduction, the four lines shift to higher fields but the shift is very small for what are assumed to be the four belt atoms furthest from the molybdenum atoms. Kozik et al. [128] have claimed that the electrons are evenly distributed over the six Mo atoms. None of the shifts exceeds -30 ppm and there is not enough data to support delocalization and ring currents in the system.

7. Miscellaneous

In this section we will consider some incomplete and scarce results with a sometimes ambiguous interpretation of the electron distribution in large polyoxomolecules. It is hoped that the results, which are often quite interesting, might shed some light on the chemical bonding, if interpreted correctly, or will stimulate further detailed studies.

7.1. Uneven two electron distribution in HPA

HPA with one tungsten replaced by another cation may be reduced by two electrons giving rise to two different cases. In one case, the bipolaron 'feels' the presence of the guest cation, as in for example $XW_{11}M^{m+}O_{40}^{n-}$ (2e). The other case has one electron anchored by the guest cation, Mo(V) for example, and rests immobile while the other is assumed to delocalize forming different loops [127,128].

Different possibilities have been envisaged for the mode of interaction of the delocalized (?) or hopping electrons upon the shift of ^{183}W-NMR lines for the α_1- and α_2-forms of the mixed reduced forms $P_{12}W_{17}Mo^{5+}O_{62}^{8-}$ (2e). In the α_2-form the Mo^{5+} in the triplet gives rise to nine lines due to the mirror plane in both the oxidized and reduced states [128], with the nine lines having δ values from $+210$ to -235 ppm in the reduced state (Table 10). For the α_1-isomer in which the Mo replaces a tungsten in the belt, all tungstens are different and would display 17 different lines if they could be resolved. The introduction of two electrons results in 17 lines with chemical shifts between $+413$ and -309 ppm [128]. In the analysis of the shifts in both cases, it was assumed [127,128] that one electron resided on the Mo^{5+} and the second electron was delocalized over the six-member belts as shown in Scheme IX (c-belt) and Scheme X (b-belt) (see Fig. 8 for notation) (—, corner sharing; ═, edge sharing).

Estimations of the possible shifts between reduced and oxidized anions were based solely on the Mo-derivatives [128].

It is known, however, that the charge of the guest cation may increase the shift range markedly. For example in the case of the α_2-$P_2W_{17}VO_{62}^{7-}$ analog of α_2-$P_2W_{17}Mo^{5+}O_{62}^{7-}$, which lacks a d^1 electron on the vanadium, the resonances are spread over the interval from -105 to -209 ppm [120]. The resonance line assigned to the unique tungsten in the triplet group which is related to the V^{5+} by a mirror plane is observed at -165 ppm giving a -36 ppm shift from the parent anion (Table 10). Thus any estimate of the shifts should take into account such displacements due to decreased charges of the replacement cation. It is also

Table 10
The ^{183}W- and ^{31}P-NMR chemical shifts[a] for the diamagnetic Dawson anions

Anion	W_a	W_b	W_c	P_a	P_b	Ref.
$P_2W_{15}Mo_3O_{62}^{6-}$	−134	−180	−179	−10.4	−12	[70]
$P_2W_{15}Mo_3O_{62}^{8-}$ (2e)	−149	−226	−238			[95]
$P_2W_{15}V_3O_{62}^{9-}$	−157	−228	−181	−6.3	−13.9	[120]
$P_2W_{15}Nb_3O_{62}^{9-}$	−139	−209	−169	−7.2	−13.8	[125]
$P_2W_{12}Mo_6O_{62}^{6-}$	−130	−180 −167				[126]
$P_2W_{12}Mo_6O_{62}^{8-}$ (2e)	−149	−191 −171				[128]
α_2-$P_2W_{17}MoO_{62}^{6-}$	−124 −129 −130*	−170 −176	−173 −175 −178	−11.7	−12.5	[120]
α_2-$P_2W_{17}VO_{62}^{7-}$	−105 −123 −165*	−164 −184	−177 −182 −185 −209	−10.8	−12.9	[120]
α_2-$P_2W_{17}MoO_{62}^{8-}$ (2e)	210 −191* −59 (×4)	−111 −235	−180 −202	−3.8	−13.4	[128]
α_1-$P_2W_{17}MoO_{62}^{8-}$ (2e)	413 99 62 15 −22 −123 −124 −128 −175 −192 (×2) −204 −206 −209 −220 −233 −254 −309			6.3	−3.4	[128]

[a] Measured relative to $Na_2^{183}WO_4$ and $H_3^{31}PO_4$, respectively, in aqueous solutions. All W lines with intensity 1, except for those marked with * with 0.5 intensity

noteworthy, that the diamagnetic susceptibility per delocalized electron of the α_2-isomer is much larger than that of the reduced parent anion [127].

The shortest pathway for two electrons to interact (Mo–O–W) is shown by a wavy line in Schemes IX and X. It is seen in Scheme X that there are two short routes but only one in Scheme IX. Moreover in Scheme IX, there can be up to eight M–O bonds, through Mo–O–W_a–O–W_a–O–W_b–O–W_c–, needed to couple the two electrons.

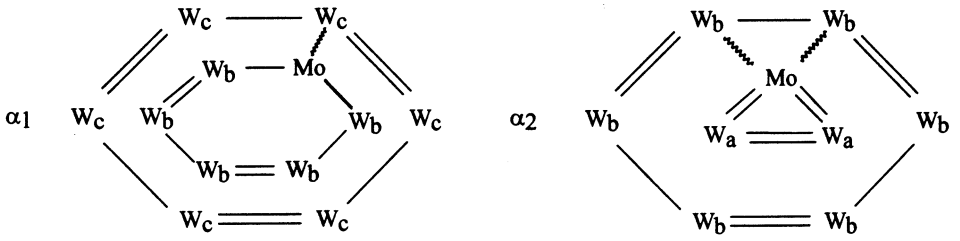

IX $P_2W_{17}MoO_{62}^{8-}$ X

Scheme IX and Scheme X.

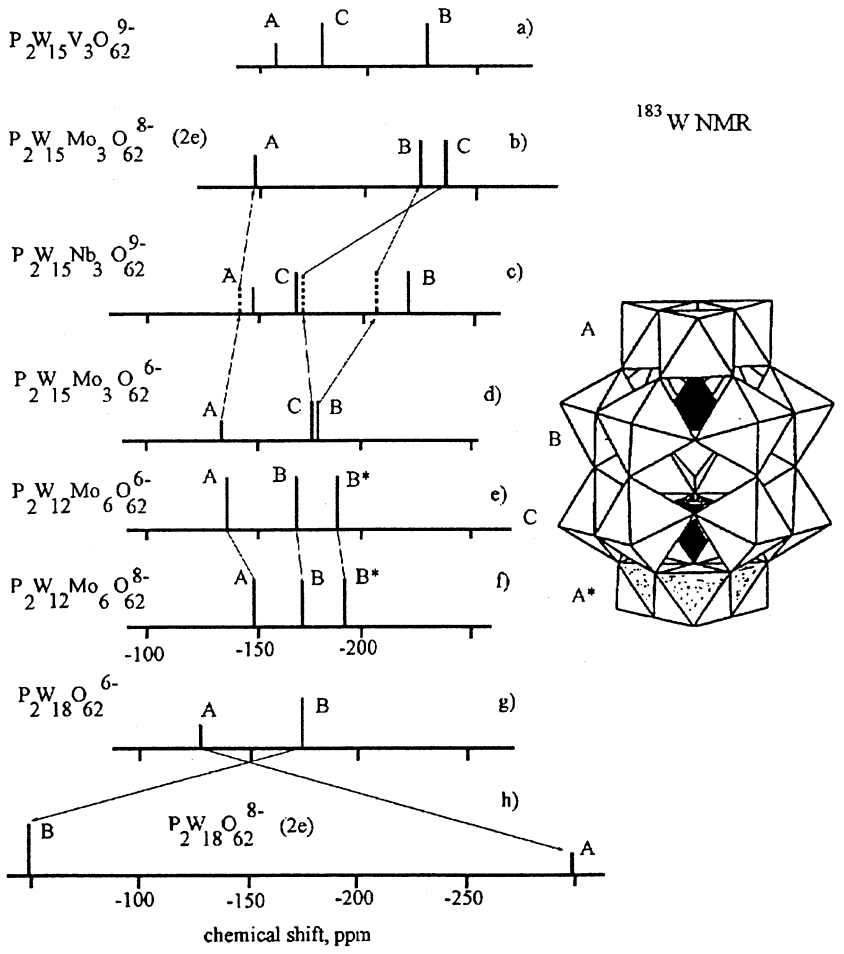

Fig. 10. The Dawson anions and ^{183}W-NMR chemical shift diagram.

We can consider another possible way to form delocalization loops which are shown in Schemes XI and XII.

In this case, however, the hopping electron should bypass the W_a atoms whose d_{xy} orbital is 4000 cm^{-1} higher than those for $W_{b,c}$ [129]. This situation may be compared, nevertheless, with $P_2W_{12}Mo_6O_{26}^{8-}$ (2e), where the electron can delocalize from the belt to the triplet. Moreover, our MO calculations on large polyoxoanions [130] show that the contribution of the Mo d_{xy} in the anion MO lowers the energy of the W d_{xy} and increases the number of pathways for coupling of two electrons, which favors this type of delocalization.

Finally, we might consider that the electron is only partly delocalized (oscillates) and the chemical shifts are induced by the ground state being delocalized on the neighboring W-atoms. For the α_2-isomer the second electron may hop between two

W_b atoms in the belt to the Mo atom by corner sharing. The estimated value of the ^{183}W-NMR shift in this case is about $+800((210-(-172)\times 2)$ ppm which is surprisingly close to the estimated $+900$ ppm for the W $5d^1$ electron in the case of complete localization.

In the α_1-isomer the much larger shift (about 419 ppm) for the tungsten atom which is adjacent to the Mo atom and related to it by a mirror plane indicates a stronger localization of the d^1 electron. However, the other positive shifts are almost the same for the two types of isomers. There is a possible ground state delocalization from the tungsten atom which is bonded by three corner sharing oxygens ensuring a high degree overlapping. It is noteworthy that one line was observed at -320 ppm, probably induced by a spin polaron, but the δ should not be compared with α_1-$PW_{17}MoO_{62}^{6-}$ but rather with α_1-$PW_{17}VO_{62}^{7-}$ to take into account the change in the charge upon reduction. This interesting problem needs further detailed investigation.

The influence of two electron currents upon the magnetic properties of HPA with paramagnetic centers was extensively studied by Baker et al. [131,132] but the NMR was done only for $Co^{2+}W_{12}O_{40}^{8-}$ (2e) [48]. The introduction of two electrons deshields the tungstens ($\Delta\delta = +338$ ppm), a magnitude much larger than the expected $\Delta\delta = +51$ ppm observed for the diamagnetic $SiW_{12}O_{40}^{6-}$ (2e). This was explained [132] by a change in the delocalization mechanism of the unpaired electron spin density from Co(II) into the W-orbitals. However, the reduced species should have a slightly longer Co–W distance, resulting from a shorter Co–O_a and a longer O_a–W bond, and this might be expected to reduce the transmission of spin density from the Co^{2+}. Certainly there should be some interaction of the unpaired spins of Co with the W $5d^1$ electron, but a quantitative estimate is not appropriate at this time. The influence of subtle changes in the dimensions of the anion induced by a central atom will result in marked changes in the ^{183}W-NMR shifts for the reduced species $XW_{12}O_{40}^{n-}$ with six electrons [133].

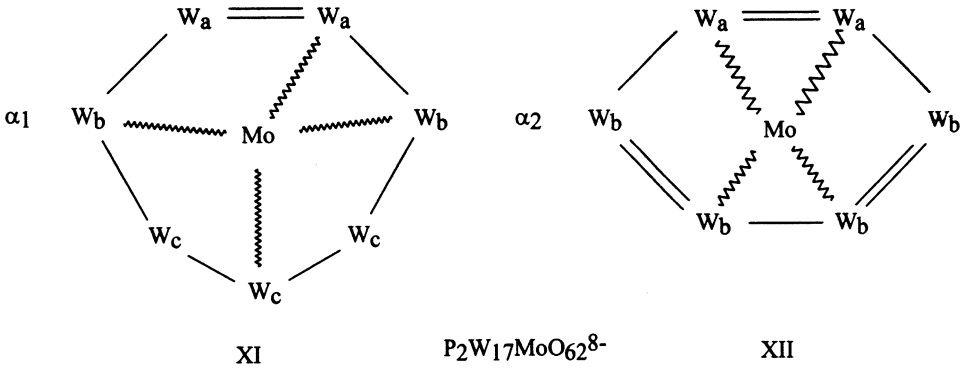

XI $P_2W_{17}MoO_{62}^{8-}$ XII

Scheme XI.

Scheme XII.

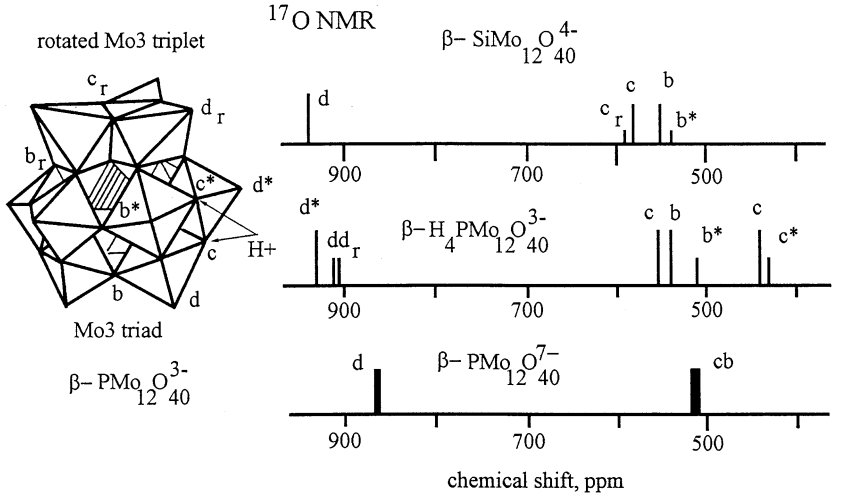

Fig. 11. α- and β-$XMo_{12}O_{40}^{n-}$ and ^{17}O-NMR chemical shift diagram.

7.2. Reduced HPA with more than two electrons

These cases will be considered briefly because the results are far from conclusive and these highly reduced species need a more systematic study.

The introduction of four electrons into $PMo_{12}O_{40}^{3-}$ results in a rather rapid isomerization of the α- into the β-form with one triplet rotated 60° [134] (Fig. 11). The high negative anionic charge may result in protonation and will affect the distribution of the electron density in the reduced anion [96,135] From X-ray single crystal analysis of the protonated four-electron reduced form it was deduced that the electrons are delocalized over a six member ring [134]. The ^{17}O-NMR of the reduced molybdophosphoric acid of the pure four-electron form [135] and a mixture of the two- and four-electron forms [96] show an uneven distribution of electron density also. In the acidic solution there are three lines with an intensity ratio of (2:1:1) with two lines shifted to high field (Fig. 11) which, at first glance, might lead one to assume delocalization of one electronic pair in the rotated triplet and the other pair in the opposite triad Mo_3, linked by corner sharing. But it should be born in mind that this anion is heavily protonated by four protons at the oxygen in the bent Mo–O–Mo bridges.

Analysis of the shifts due to protonation, increased charge, and electron delocalization permits one to conclude that electron pairs are distributed in the member ring probably on the opposite pairs of molybdenum which are separated by Mo^{6+} atoms. Deprotonation of the anion results in a redistribution of the electron pairs with some or most of the electron density passed onto the molybdenum atoms in the triplet and triad. So the protonated octahedra serves as an 'electron sink' for the electron density. Unfortunately the line width does not allow for a making more definitive conclusions.

A detailed electrochemical study of the reduction of the metatungstate $H_2W_{12}O_{40}^{6-}$ by Launay [136] has shown that the anion may reversibly accept up to 36 electrons. In the case of six electrons (six electrons on tungstens) an electronic isomerization takes place with the electrons localized in three W^{IV} $4d^2$ centers. This was proven by ESCA [137] and by the large ^{183}W-NMR shifts which exhibit $^2J_{W-W}$ couplings of the magnitude expected for a metal–metal bond [138]. The insensitivity of the nearby tungstens to the presence of the d^2 electrons indicates that the electrons are firmly trapped. A weak negative shift for the NMR lines of ^{17}O for atoms linking the W^{IV} and W^{IV} might indicate a small delocalization but a slight elongation of the W^{IV}–O–W^{IV} bonds is a more probable explanation. Analysis of the spin–spin coupling $^2J_{w-w}$ shows that the six electrons are located in the triplet of edge shared octahedra. Detailed X-ray single crystal study on six electron-reduced $BW_{12}O_{40}^{5-}$ has shown the localization of six electrons in the such a triplet as well [139].

7.3. Delocalization of unpaired and paired t_{2g} electrons

The rather simple anions $M^{m+}Mo_6O_{24}H_6^{n-}$ are built of six edged shared octahedra forming a ring around the central atom M^{m+} with an octahedral configuration [5]. Each MoO_6 octahedron is distorted to C_{2v} symmetry with two *cis*-terminal oxygens which make two empty π-orbitals which are slightly antibonding (see Scheme II). The oxygens in the XO_6 form bonds with the two Mo atoms and are protonated in the case of $m = 2$ or 3.

For Al^{III}, Ga^{III}, Te^{VI}, and I^{VII} The ^{95}Mo-NMR chemical shifts are in a narrow range [104,140] (Table 11). The influence of Cr^{3+} (d^3 in t_{2g} orbitals) is very small on the Mo atoms but the terminal and bridging oxygens are shifted [141]. In contrast to $Co^{2+}W_{12}O_{40}^{6-}$ where the terminal and bridging oxygens are deshielded (Table 4), the terminal oxygens of $Cr(OH)_6Mo_6O_{18}^{3-}$ are deshielded and the bridging Mo–O–Mo are shielded. According to the calculated *G* values for the

Table 11
The ^{17}O- and ^{95}Mo-NMR chemical shifts[a] for heteropolymolybdates $XMo_6O_{18}^{n-}$ and other anions

X	O_d	O_c	O_a	Mo	Ref.
$Al^{III}(OH)_6$	834	377		−21	[104,140]
$Ga^{III}(OH)_6$	834	373		−3	[140]
$Te^{VI}O_6$	807	383	180	10	[104,140]
$I^{VII}O_6$	825	357	255	−11	[104,140]
$Cr^{III}(OH)_6$	893	318		−14	[141]
$Co^{III}(OH)_6$	836	376		60	[141]
G	0.009	0.021		0.025	
$Co_2^{III}Mo_{10}O_{36}H_4^{6-}$	877 855 846 811	395	382 −57 850	153 47	[141]
$Ni^{IV}Mo_9O_{32}^{6-}$	868 862	401	201	87 63	[82]

[a] Measured in aqueous solutions relative to $H_2^{17}O$ and $Na_2^{95}MoO_4$.

dipolar shift contribution for an anion possessing D_{3d} symmetry both types of oxygens and the molybdenum should experience shifts of the same sign (Table 11). This contribution should be twice as large for the bridging oxygens.

The three electrons in t_{2g} orbitals interact mainly through the π-orbitals of molybdenum and the p_π-orbitals of oxygen. The presence of the electron density in them will induce a negative spin density at the nucleus of the molybdenum and oxygen atoms resulting in a deshielding of the nucleus. The amount of spin density can only be estimated from MO calculations. To this contact contribution must be added the dipolar contribution to the shift. Unfortunately there are no atoms which can be regarded as free from the contact interaction to use in estimating the dipolar contribution of the shift.

Co^{3+} with its spin paired d^6 electrons shows a marked positive shift of the ^{95}Mo line ($\delta = +60$ ppm) which is unusual for this type of anion [141]. Thus it may be assumed that some unusual electron density is transferred through the bridges $Co\langle{}^{O}_{O}\rangle Mo$, though the resonance from these oxygens could not be observed.

The assumption of electron density transmission from cobalt may be confirmed by the ^{95}Mo-NMR of the dimeric $Co_2Mo_{10}O_{32}H_4^{4-}$ which shows two lines of the deshielded molybdenum (Table 11). It should be noted that the line from the oxygen linking Co^{III} and Mo is also shifted to -57 ppm. This shielding may be compared with the shift that is observed for the two electron reduced forms where tungsten is deshielded and oxygen is shielded (Table 8).

Finally, $Ni^{4+}Mo_9O_{32}^{6-}$ with spin paired d^6 electrons and an octahedral configuration about Ni^{IV} (see Section 4.2) gives well resolved ^{17}O- and ^{95}Mo-NMR spectra [82]. Two lines in the latter compound are shifted to low field indicating possible delocalization of the d^6 electrons onto molybdenum.

A more complex electron density distribution may be expected when HPA contains two or more paramagnetic cations. Sometimes the magnetic properties of such complexes are markedly different [131,132] and the behavior of the NMR lines is not predictable. For example for $A–SiW_9Co_3O_{40}^{n-}$ where three Co^{II} atoms make up a three corner-shared triad, two ^{183}W lines with a large positive shift ($+708$ ppm) and one negative (-690 ppm) shift are observed and assigned respectively to tungstens non-bonded and bonded to Co^{II}, which broadens the resonance of the latter [142].

Delocalization of paramagnetic electrons from a Cu-triad of β-$SiW_9O_{37}CuR$ over protons of pyridine and picoline coordinated to copper have been studied by ^1H-NMR. The isotropic shifts result mainly from the contact interaction [143].

And finally we should mention complexes which contain atoms with a lone pair of p electrons. Though usually this lone pair is directed outwards from the polyanion as in $PW_{11}O_{39}Pb(II)^{5-}$, some kind of influence can be assumed from the position of the ^{183}W lines of the adjacent tungsten atoms [144]. In comparison with other complexes where the cation (Ln) rests on the surface of $PW_{11}O_{39}$ or W_5O_{18} ligands whose ^{183}W lines experience negative shifts in the Pb complex, the adjacent W atoms experience deshielding as if the π-electron density passed onto these tungstens. However this assumption should be verified with other complexes and using ^{17}O-NMR as well. Noteworthy in the ^{183}W-NMR spectrum of the dimeric

complex $[Sn_3^{II}(PW_9O_{34})_2]^{12-}$ is the line assigned to the tungsten adjacent to tin (II) which is observed in the low field region, but in the oxidized complex with Sn(IV) this line is shifted to high fields [145]. Though some structural changes do occur in the oxidized form, the influence of the lone pair, along with structural changes, might affect the position of the NMR lines.

8. Conclusions

In a discussion of NMR and EPR of conventional complexes with paramagnetic centers, Eaton and Zaw [146] noted that "there is and obvious symmetry to the two approaches". EPR probes the metal ion with unpaired spins and the influence of its immediate environs, and NMR studies the changes in the ligand and sometimes of the central atoms due to complex formation. HPA studies are quite unique in allowing us to study, in many cases as we have shown, the same systems by both complementary methods.

This review is written to draw attention to some problems which have a great significance both in fundamental research and in the applied fields. Analysis of the results presented here is far from conclusive, but attempts to get self-consistent conclusions have been made.

It is shown that the electron transfer includes π and σ pathways and that there is a large contact contribution induced by unpaired electrons. The geometry and symmetry of HPA are clearly manifested in the ^{183}W-NMR spectra and the presence of the unpaired spins strongly amplify the shift differences. In some cases two large contact contributions with opposite signs from the different s-orbitals of the nucleus under question may result in a small isotropic shift. Though ligand centered contributions may reach rather sizable values, its presence should be verified by independent measurements.

EPR and NMR confirm a great mobility of a single electron through the bonds in HPA. The second electron is completely paired with the first one if there is a possibility of their delocalization or the formation of a bipolaron. Perhaps two electrons immobilized on adjacent metal atoms are coupled by a weak antiferromagnetic coupling. It would seem that the bipolaron and/or spin polaron have been shown experimentally by NMR spectroscopy for the first time. Moreover, delocalization of the spin-paired electrons from the diamagnetic cation opens new dimensions for NMR spectroscopy.

The theory of NMR of paramagnetic and diamagnetic polyoxo complexes with delocalized electrons is in the dawn of development. And though Fontenelle wrote that "the understanding is important, not the quantities", the quantitative estimation of the electron density distribution is highly desirable for an understanding of the electronic structure of such complex oxide systems.

It is hoped the available results and the discussion presented here will be useful in further studies to account for all possible ways of influencing the spin distribution parameters of EPR and NMR.

References

[1] M.T. Pope, in: G. Wilkinson, R.D. Gillard, J.A. McCleverty (Eds.), Comprehensive Coordination Chemistry, vol. 3, Pergamon, Oxford, 1987, p. 1023.
[2] M.T. Pope, A. Müller, Angew. Chem. Int. Ed. Engl. 30 (1991) 34.
[3] M.T. Pope, A. Mtller (Eds.), Polyoxometalates: From Platonic Solids to Anti-retroviral Activity, Kluwer Academic, Dordrecht, 1993.
[4] M.A. Fedotov, NMR in Solutions of Inorganic Componds (in Russian), Nauka, Novosibirsk, 1986.
[5] M.T. Pope, Isopoly and Heteropoly Metalates, Springer-Verlag, Berlin, 1983.
[6] P. Chaquin, M. Fournier, G. Herve, L.P. Kazansky, Polyhedron (submitted for publication).
[7] C.J. Ballhausen, H.B. Gray, Inorg. Chem. 1 (1962) 111.
[8] L.P. Kazansky, J. Chim. Phys. 91 (1994) 341.
[9] C.J. Jameson, J. Mason, in: J. Mason (Ed.), Multinuclear NMR, Plenum Press, New York, 1987.
[10] L.P. Kazanskii, Koordin. Khim. 3 (1977) 327.
[11] R. Acerete, C.F. Hammer, L.C.W. Baker, J. Am. Chem. Soc. 103 (1982) 5384.
[12] C. Brevard, R. Schimpf, G. Tourne, C.M. Tourne, J. Am. Chem. Soc. 105 (1983) 7059.
[13] V.I. Spitsyn, L. Kazansky, E.A. Torchenkova, Sov. Sci. Rev. Sec. B, 181, 3 (1981) 111.
[14] T.L. Jorris, M. Kozik, N. Casan-Pastor, P.J. Domaille, R.G. Finke, W.K. Miller, L.C.W. Baker, J. Am. Chem. Soc. 109 (1987) 7402.
[15] C.P. Jesson, in: G. Lamar, W. Horrocks, R.H. Holm (Eds.), NMR of Paramagnetic Molecules, Academic Press, New York, 1983.
[16] B.R. McGarvey, Inorg. Chem. 34 (1995) 6000.
[17] R.M. Golding, M.P. Halton, Austr. J. Chem. 25 (1972) 2577.
[18] R.J. Kurland, B.R. McGarvey, J. Magn. Res. 2 (1970) 286.
[19] B. Bleaney, J. Magn. Res. 8 (1972) 91.
[20] G.A.Webb, in: E.F.Mooney (Ed.), Annual Reports on NMR Spectroscopy 6A, 1975, pp. 1–130.
[21] I. Bertini, C. Luchinato, Coord. Chem. Rev. 150 (1996) 1.
[22] R.S. Drago, Physical Methods In Chemistry, Saunders, Philadelphia, PA, 1977.
[23] J.P. Launay, in: G.J. Long, F. Grandjean (Eds.), The Time Domain in Surface and Structural Dynamics, Kluwer Academic, Dordrecht, 1988, p. 233.
[24] H. So, M.T. Pope, in: Muller et al., Electron and Proton transfer in Chemistry and Biology, vol. 78, 1992, p. 71.
[25] C. Sanchez, J. Livage, J.P. Launay, M. Fournier, Y. Jeannin, J. Am. Chem. Soc. 104 (1982) 3194.
[26] C. Sanchez, J. Livage, J.P. Launay, M. Fournier, J. Am. Chem. Soc. 105 (1982) 6817.
[27] M.M. Mossoba, C.J. O'Connor, M.T. Pope, E. Sinn, G. Herve, A. Teze, J. Am. Chem. Soc. 102 (1980) 6864.
[28] (a) H. So, C.W. Lee, Bull. Korean Chem. Soc. 11 (1990) 115. (b) H. So, C.W. Lee, Bull. Korean Chem. Soc. 7 (1986) 318.
[29] S.P. Harmalker, M.A. Leparulo, M.T. Pope, J. Am. Chem. Soc. 105 (1983) 4286.
[30] H. So, C.W. Lee, D. Lee, Bull. Korean Chem. Soc. 8 (1987) 384.
[31] E. Cadot, M. Fournier, A. Teze, G. Herve, Inorg. Chem. 35 (1996) 282.
[32] G. Lamar, W. Horrocks, R.H. Holm (Eds.), NMR of Paramagnetic Molecules, Academic Press, New York, 1983.
[33] D.D. Dexter, I.V. Silverton, J. Am. Chem. Soc. 90 (1968) 3589.
[34] I.V. Tatianina, V.N. Molchanov, V.M. Ionov, E.A. Torchenkova, V.I. Spitsyn, Izv. Akad. Nauk. Ser. Khim. (1982) 803.
[35] M.K. Kotvanova, M.A. Fedotov, L.P. Kazanskii, E.A. Torchenkova, Koordin. Khim. 10 (1984) 1063.
[36] I.V. Tatianina, V.N. Molchanov, E.A. Torchenkova, L.P. Kazanskii, Koordin. Khim. 8 (1982) 1261.
[37] M. Alizadeh, S.P. Harmalker, Y. Jeannin, J. Martin-Frere, M.T. Pope, J. Am. Chem. Soc. 107 (1985) 2662.

[38] J. Iball, T.J.R. Weakley, J. Chem. Soc. Dalton Trans. (1974) 2021.
[39] A.M. Golubev, L.P. Kazanskii, E.A. Torchenkova, V.I. Spitsyn, Dokl. Akad. Nauk. SSSR 221 (1975) 351.
[40] T. Ozeki, T. Yamase, Acta Crystallogr. B50 (1994) 128.
[41] (a) I. Creaser, M.C. Hechel, R.J. Neitz, M.T. Pope, Inorg. Chem. 32 (1993) 1573. (b) M.H. Dickman, G.J. Gama, K. Kim, M.T. Pope, J. Cluster Sci. 7 (1996) 567.
[42] M.A. Fedotov, L.P. Kazanskii, V.I. Spitsyn, Dokl. Akad. Nauk. SSSR 272 (1983) 1179.
[43] M.A. Fedotov, E.P. Samokhvalova, L.P. Kazanskii, Koordin. Khim. 22 (1996) 219.
[44] M.A. Fedotov, E.P. Samokhvalova, E.A. Torchenkova, Izv. Sib. Otd. Akad. Nauk. SSSR 6 (1989) 42.
[45] M.A. Fedotov, E.P. Samokhvalova, L.P. Kazansky, Polyhedron 15 (1996) 2241.
[46] J. Bartis, S. Sukal, M. Dankova, E. Kraft, R. Kronzon, M. Blumstein, L.C. Francesconi, J. Chem. Soc. Dalton Trans. (1997) 1937.
[47] L.P. Kazanskii, A.M. Golubev, I.I. Baburina, E.A. Torchenkova, V.I. Spitsyn, Izv.Akad. Nauk. SSSR Ser. Khim. (1978) 2215.
[48] N. Casan-Pastor, P. Gomez-Romero, C.B. Jameson, L.C.W. Baker, J. Am. Chem. Soc. 113 (1991) 5658.
[49] V.E. Simmons, Diss. Abstr. Int. 29b (1977) 926.
[50] L.P. Kazanskii, M.A. Fedotov, Koordin. Khim. 14 (1988) 939.
[51] B.R. McGarvey, J. Magn. Res. 33 (1978) 448.
[52] R. Acerete, N. Casan-Pastor, J. Bas-Serra, L.C.W. Baker, J. Am. Chem. Soc. 111 (1989) 6049.
[53] V.S. ergienko, M.A. Porai-Koshits, E.N. Yurchenko, Zh. Strukt. Khim. 21 (1980) 111.
[54] J. Fuchs, A. Tiele, R. Palm, Angew. Chem. Int. Ed. Engl. 23 (1982) 789.
[55] H.T. Evans, M.T. Pope, Inorg. Chem. 23 (1984) 501.
[56] P.R. Sethuraman, M.A. Leparulo, M.T. Pope, F. Zonnevijlle, C. Breward, J. Lemerle, J. Am. Chem. Soc. 103 (1981) 7665.
[57] P.J. Domaille, G. Watunya, Inorg. Chem. 25 (1986) 1239.
[58] O.W. Howarth, P. Kelly, J. Chem. Soc. Chem. Commun. (1988) 1236.
[59] L.P. Kazansky, M.A. Fedotov, J. Chem. Soc. Chem. Commun. (1983) 417.
[60] C. Tourne, G. Tourne, M. Brianso, Acta Crystallogr. B36 (1980) 2012.
[61] V.N. Molchanov, L.P. Kazansky, E.A. Torchenkova, V.I. Simonov, Sov. Phys. Crystallogr. 24 (1979) 96.
[62] M.A. Fedotov, V.N. Molchanov, L.P. Kazanskii, E.A. Torchenkova, V.I. Spitsyn, Dokl. Akad. Nauk. SSSR 237 (1979) 245.
[63] M.A. Fedotov, B.Z. Pertsikov, D.K. Danovich, Koordin. Khim. 7 (1991) 234.
[64] M.A. Fedotov, B.Z. Pertsikov, D.K. Danovich, Polyhedron 9 (1990) 1249.
[65] J.F. Kirby, L.C.W. Baker, J. Am. Chem. Soc. 117 (1885) 10010.
[66] M.A. Fedotov, L.G. Detusheva, L.I. Kuznetsova, V.A. Likholobov, Zh. Neorg. Khim. 38 (1992) 515.
[67] R.L. Kravchenko, M.A. Fedotov, R.I. Maksimovskaya, L.I. Kuznetsova, Zh. Neorg. Chim. 39 (1994) 629.
[68] C. Rong, M.T. Pope, J. Am. Chem. Soc. 114 (1992) 293.
[69] A. Proust, M. Fournier, R. Thouvenot, P. Gousehr, Inorg. Chim. Acta 215 (1994) 619.
[70] M. Kozik, C.F. Hammer, L.C.W. Baker, J. Am. Chem. Soc. 108 (1986) 7627.
[71] H. D'Amour, Acta Crystallogr. B32 (1976) 729.
[72] V.S. Sergienko, M.A. Porai-Koshits, S.V. Kiselev, N.A. Butman, V.F. Chuvaev, Zh. Neorg. Khim. 38 (1983) 1197.
[73] M. Ko, G.I. Rhiu, H. So, Bull. Korean Chem. Soc. 14 (1993) 500 673.
[74] D. Doddrell, J.D. Roberts, J. Am. Chem. Soc. 92 (1970) 4484.
[75] M.A. Fedotov, L.P. Kazanskii, Koordin. Khim. 10 (1984) 423.
[76] E.P. Samokhvalova, V.N. Molchanov, I.V. Tatianina, E.A. Torchenkova, Koordinat. Khim. 16 (1990) 207.
[77] E.P. Samokhvalova, V.N. Molchanov, I.V. Tatianina, E.A. Torchenkova, Koordinat. Khim. 16 (1990) 1277.

[78] M.A. Petrukhina, V.M.I onov, A.E. Prozorovskii, V.N. Molchanov, I.V. Tatianina, E.A. Torchenkova, Koordinat. Khim. 14 (1988) 1519.
[79] E.P. Samokhvalova, M.A. Fedotov, I.V. Tatianina, E.A. Torchenkova, Zh. Neorg. Khim. 35 (1990) 2104.
[80] M.A. Petrukhina, M.A. Fedotov, I.V. Tatianina, E.A. Torchenkova, Zh. Neorg. Khim. 34 (1989) 3118.
[81] M.A. Petrukhina, M.A. Fedotov, I.V. Tatianina, E.A. Torchenkova, Zh. Neorg. Khim. 35 (1990) 2110.
[82] K.O. Gavrilova, M.A. Fedotov, I.V. Tatianina, E.A. Torchenkova, Zh. Neorg. Khim. 35 (1990) 2100.
[83] A. Proust, R. Thouvenot, S.G. Roh, J.K. You, P. Gouzerh, Inorg. Chem. 34 (1995) 4106.
[84] P.J. Domaille, J. Am. Chem. Soc. 106 (1984) 7677.
[85] J.P. Launay, Polyoxometallate Workshop, St. Lambert des Bois, France, 1983.
[86] M.A. Filowitz, R.K. Ho, W.G. Klemperer, Inorg. Chem. 18 (1979) 93.
[87] K. Piepgrass, J.N. Barrows, M.T. Pope, J. Chem. Soc. Chem. Commun. (1989) 10.
[88] J.P. Launay, M. Fournier, C. Sanchez, J. Livage, M.T. Pope, Inorg. Nucl. Chem. Lett. 16 (1980) 257.
[89] R.A. Prados, M.T. Pope, Inorg. Chem. 15 (1976) 2547.
[90] J.J. Altenau, M.T. Pope, R.A. Prados, H. So, Inorg. Chem. 14 (1975) 417.
[91] I.V. Potapova, T.A. Karpukhina, L.P. Kazanskii, V.I. Spitsyn, Izv. Akad. Nauk. SSSR Ser. Khim. (1979) 724.
[92] C. Sanchez, M. Michaud, J. Lavage, G. Herve, J. Inorg. Nucl. Chem. 43 (1981) 2795.
[93] E. Cadot, R. Thouvenot, A. Teze, G. Herve, Inorg. Chem. 31 (1992) 4128.
[94] L.P. Kazansky, Chem. Phys. Lett. 223 (1994) 289.
[95] M. Fournier, C. Rocchiccioli-Deltcheff, L.P. Kazansky, Chem. Phys. Lett. 223 (1994) 297.
[96] L.P. Kazansky, M.A. Fedotov, I.V. Potapova, V.I. Spitsyn, Dokl. Akad. Nauk. SSSR 244 (1979) 372.
[97] J. Barrows, M.T. Pope, Adv. Chem. Ser. 6 (1990) 403.
[98] L.P. Kazansky, I.V. Potapova, V.I. Spitsym, in: Proceedings of the 3rd International Conference on the Chemistry and Uses of Mo and W, Ann Arbor, USA, 1979, p. 67.
[99] C. Sanchez, J. Livage, P. Doppelt, F. Chauveau, J. Lefebvre, J. Chem. Soc. Dalton Trans. (1982) 2425.
[100] D. Gourier, P. Doppelt, C. Sanchez, Inorg. Chem. 25 (1986) 4462.
[101] S.S. Zhu, B. Xue, X.Q. Shi, Y.D.J. Liu, M.Q. Che, V.F. Huang, J. Chem. Soc. Dalton Trans. (1993) 3633.
[102] Y. Jeannin, J.P. Launay, C. Sanchez, J. Livage, M. Fournier, Nouv. J. Chim. 4 (1980) 587.
[103] J. Barrows, M.T. Pope, Inorg. Chim. Acta 213 (1993) 91.
[104] M.A. Fedotov, Izv.Akad. Nauk. SSSR Ser. Khim. (1984) 1166.
[105] J.B. Cooper, D.M. Way, A.M. Bond, A.G. Wedd, Inorg. Chem. 32 (1993) 2416.
[106] U. Kortz, M.T. Pope, Inorg. Chem. 33 (1994) 3643.
[107] M. Kozik, C.F. Hammer, L.C.W. Baker, J. Am. Chem. Soc. 108 (1986) 2748.
[108] E.K.H. Salje, Eur. J. Solid State Inorg. Chem. 31 (1994) 805.
[109] J. Park, H. So, Bull. Korean. Chem. Soc. 15 (1994) 752.
[110] E. Cadot, V. Bereau, B. Marg, S. Halut, F. Secheress, Inorg. Chem. 35 (1996) 3099.
[111] M. Kozik, L.C.W. Baker, J. Am. Chem. Soc. 109 (1987) 3159.
[112] S.A. Borsch, J.-J. Girerd, Chem. Phys. 181 (1994) 1.
[113] L.P. Kazansky, M.A. Fedotov, V.I. Spitsyn, Dokl. Akad. Nauk. SSSR 233 (1977) 152.
[114] A. Teze, K. Canny, L. Gourban, R. Thovenot, G. Herve, Inorg. Chem. 35 (1996) 1001.
[115] M.A. Fedotov, L.P. Kazansky, V.I. Spitsyn, Dokl. Akad. Nauk. SSSR 272 (1983) 1179.
[116] T. Yamase, T. Usami, J. Chem. Soc. Dalton. Trans. (1988) 185.
[117] D.C. Duncan, C.L. Hill, Inorg. Chem. 35 (1996) 5828.
[118] A. Chemseddine, C. Sanchez, J. Livage, J.P. Launay, M. Fournier, Inorg. Chem. 2 (1984) 2609.
[119] T. Yamase, J. Chem. Soc. Dalton Trans. (1987) 1597.
[120] M. Abessi, R. Contant, R. Thouvenot, G. Herve, Inorg. Chem. 30 (1991) 1695.

[121] L.P. Kazansky, Chem. Phys. Lett. 258 (1996) 248.
[122] N. Mott, Phil. Mag. B. 65 (1992) 767.
[123] L.P. Kazansky, M.A. Fedotov, J. Chem. Soc. Chem. Commun. (1980) 644.
[124] J.F. Garvey, M.T. Pope, Inorg. Chem. 17 (1978) 1115.
[125] D.J. Edlund, R.J. Saxton, D.K. Lyon, R.G. Finke, Organometallics 7 (1988) 1692.
[126] M. Kozik, N. Casan-Pastor, C.F. Hammer, L.C.W. Baker, J. Am. Chem. Soc. 111 (1988) 7697.
[127] R. Acerete, C.F. Hammer, L.C.W. Baker, Inorg. Chem. 23 (1984) 1478.
[128] M. Kozik, L.C.W. Baker, in: M.T. Pope, A. Muller (Eds.), Polyoxometalates: From Platonic to Anti-retroviral Activity, Kluwer Academic, Dordrecht, 1993, p. 191.
[129] E. Papaconstantinou, M.T. Pope, Inorg. Chem. 9 (1970) 667.
[130] P. Chaquin, M. Fournier, G. Herve, L.P. Kazansky, unpublished results.
[131] N. Casan-Pastor, L.C.W. Baker, J. Am. Chem. Soc. 114 (1992) 10384.
[132] N. Casan-Pastor, L.C.W. Baker, in: M.T. Pope, A. Muller (Eds.), Polyoxometalates: From Platonic to Anti-retroviral Activity, Kluver Academic, Dordrecht, 1993, p. 203.
[133] K. Piepgrass, M.T. Pope, J. Am. Chem. Soc. 109 (1987) 1586.
[134] J.N. Barrows, G.B. Jameson, M.T. Pope, J. Am. Chem. Soc. 107 (1981) 1771.
[135] J.N. Barrows, M.T. Pope, Adv. Chem. Ser. 226 (1990) 403.
[136] J.P. Launay, J. Inorg. Nucl. Chem. 38 (1976) 807.
[137] L.P. Kazansky, J.P. Launay, Chem. Phys. Lett. 51 (1977) 242.
[138] K. Piepgrass, M.T. Pope, J. Am. Chem. Soc. 111 (1989) 753.
[139] T. Yamase, E. Ishikawa, J. Chem. Soc. Dalton Trans. (1996) 1619.
[140] S.F. Gheller, M. Sidney, A.F. Masters, A.G. Wedd, Austr. J. Chem. 37 (1984) 1825.
[141] M.A. Fedotov, L.O. Gavrilova, I.V. Tatianina, E.A. Torchenkova, Zh. Neorg. Khim. 36 (1991) 194.
[142] J. Liu, F. Ortega, P. Sethuraman, D.E. Katsulis, C.E. Costello, M.T. Pope, J. Chem. Soc. Dalton Trans. (1992) 1901.
[143] H.Y. Woo, H. So, M.T. Pope, J. Am. Chem. Soc. 118 (1996) 621.
[144] C. Brevard, R. Schimpf, G. Tourne, C.M. Tourne, J. Am. Chem. Soc. 105 (1983) 7059.
[145] F. Xin, M. Pope, J. Am. Chem. Soc. 118 (1997) 5531.
[146] D.R. Eaton, K. Zaw, Coord. Chem. Rev. 7 (1971) 197.